AFRL-AFOSR-VA-TR-2022-0041

Microstructural Instabilities in Single Crystal Metals for Extreme Environments

Le Graverend, Jean-Briac
TEXAS ENGINEERING EXPERIMENT STATION COLLEGE STATION
1470 WILLIAM D FITCH PKY
COLLEGE STATION, TX,
US

09/27/2021
Final Technical Report

Air Force Research Laboratory
Air Force Office of Scientific Research
Arlington, Virginia 22203
Air Force Materiel Command

REPORT DOCUMENTATION PAGE

Form Approved
OMB No. 0704-0188

1. REPORT DATE *(DD-MM-YYYY)*	**2. REPORT TYPE**	**3. DATES COVERED** *(From - To)*
27-09-2021	Final	01 Apr 2017 - 31 Mar 2021

4. TITLE AND SUBTITLE
Microstructural Instabilities in Single Crystal Metals for Extreme Environments

5a. CONTRACT NUMBER

5b. GRANT NUMBER
FA9550-17-1-0233

5c. PROGRAM ELEMENT NUMBER
61102F

6. AUTHOR(S)
Jean-Briac Le Graverend

5d. PROJECT NUMBER

5e. TASK NUMBER

5f. WORK UNIT NUMBER

7. PERFORMING ORGANIZATION NAME(S) AND ADDRESS(ES)
TEXAS ENGINEERING EXPERIMENT STATION COLLEGE STATION
1470 WILLIAM D FITCH PKY
COLLEGE STATION, TX
US

8. PERFORMING ORGANIZATION REPORT NUMBER

9. SPONSORING/MONITORING AGENCY NAME(S) AND ADDRESS(ES)
AF Office of Scientific Research
875 N. Randolph St. Room 3112
Arlington, VA 22203

10. SPONSOR/MONITOR'S ACRONYM(S)
AFRL/AFOSR RTA1

11. SPONSOR/MONITOR'S REPORT NUMBER(S)
AFRL-AFOSR-VA-TR-2022-0041

12. DISTRIBUTION/AVAILABILITY STATEMENT
A Distribution Unlimited: PB Public Release

13. SUPPLEMENTARY NOTES

14. ABSTRACT
As the US Air Force fleet continues to age, a greater portion of its budget will be required to ensure safe and effective operations beyond the design service life. In fact, for various military vehicles and platforms, the recommended service life for safe operation is projected to increase by a factor of 1.5 to 5 (AFRL, 2014). The high demand for safety and cost reduction culminates in the case of materials systems operating under extreme environments such as turbine blades made of Ni-based single crystal superalloys. Turbine blades are used in the hot section of the engine and are, therefore, subjected to multiaxial high-temperature viscoplastic deformations, namely, creep and dwell/fatigue, due to both their complex geometry and their advanced design, e.g., internal cooling channels aimed to increase the exhaust-gas temperature during in-service operations.

15. SUBJECT TERMS

16. SECURITY CLASSIFICATION OF:			**17. LIMITATION OF ABSTRACT**	**18. NUMBER OF PAGES**	**19a. NAME OF RESPONSIBLE PERSON**
a. REPORT	**b. ABSTRACT**	**c. THIS PAGE**			MARTIN SCHMIDT
U	U	U	UU	26	**19b. TELEPHONE NUMBER** *(Include area code)* 588-8436

Standard Form 298 (Rev.8/98)
Prescribed by ANSI Std. Z39.18

AFOSR Final Report for the Award Number FA9550-17-1-0233

MICROSTRUCTURAL INSTABILITIES IN SINGLE CRYSTAL METALS FOR EXTREME ENVIRONMENTS

Jean-Briac le Graverend, PhD
Assistant Professor, Aerospace Engineering
Texas A&M University
TAMU 3141, College Station, TX 77843, USA

Period of performance: March 2017- March 2021

I. Introduction

As the US Air Force fleet continues to age, a greater portion of its budget will be required to ensure safe and effective operations beyond the design service life. In fact, for various military vehicles and platforms, the recommended service life for safe operation is projected to increase by a factor of 1.5 to 5 (AFRL, 2014). The high demand for safety and cost reduction culminates in the case of materials systems operating under extreme environments such as turbine blades made of Ni-based single crystal superalloys. Turbine blades are used in the hot section of the engine and are, therefore, subjected to multiaxial high-temperature viscoplastic deformations, namely, creep and dwell/fatigue, due to both their complex geometry and their advanced design, e.g., internal cooling channels aimed to increase the exhaust-gas temperature during in-service operations. Uniaxial thermo-mechanical environments have already been shown to lead to phase transformations (le Graverend et al., 2010), microstructure gradients (Ignat et al., 1993), and lattice rotations (Ardakani et al., 1999) which dramatically alter the mechanical properties. So, the following question is raised: how does in-service thermo-mechanical loading modify the kinetics of microstructural instabilities? The development of predictive deformation and damage models tailored for such extreme conditions are necessary and has recently been emphasized through the Digital Twin (DT) paradigm for future NASA and Air Force vehicles (Glaessgen and Stargel, 2012; Tuegel et al., 2011). Therefore, synergetic experimental and modeling approaches are required to step toward a fully integrated computational materials engineering. The project aimed at investigating the effects of multiaxiality and anisotropy on the kinetics of microstructural instabilities in single-crystal metals and alloys under creep.

II. Summary of Accomplishments

Key results of the project included **1**) correlating damage and topological inversion depending on the volume fraction of the strengthening phase (Harikrishnan and le Graverend, 2018), **2**) determining the role played by the lattice misfit and the microstructural state on the internal stresses (le Graverend and Harikrishnan, 2019, 2021), **3**) modeling the effect of oxidation on lifetime (le Graverend and Lee, 2020a; le Graverend and Lee, 2020b), **4**) developing a damage model for non-isothermal loading (le Graverend, 2019), **5**) determining the effect of multiaxiality on stress redistributions and lifetime (Harikrishnan et al., 2021), **6**) formulating a crystallography-sensitive phase-field model (Harikrishnan and le Graverend, 2021), **7**) formulating a phase-field-

informed vectorial modeling of rafting in Ni-based single crystal superalloys (le Graverend and (Harikrishnan, 2021). Results from each of these studies are summarized in the next sections.

II.1 PREDICTION OF TOPOLOGICAL INVERSION VIA DAMAGE-COUPLED PHASE-FIELD SIMULATIONS

A phase-field framework has been modified to mimic the effect of dislocations on the γ' phase to predict the topological inversion that occurs in the tertiary creep stage. The study aimed at better predicting the microstructural evolution of Ni-based single crystal superalloys during high-temperature/low-stress creep experiments using a newly proposed *Creep-Damage Phase-Field Model* that accounts for microstructural degradation as damage. In this context, for the first time, the complete microstructural evolution, including the topological inversion, is simulated using a phase-field model.

A damage density function, M_D evolving from 0 (undamaged state) to 1 (fully damaged state), can be interpreted as the amount of dislocations in the strengthening phase γ' and not as a conventional mechanical damage. According to the effective stress concept, the constitutive equations of any damaged material can be obtained by replacing the Cauchy stress in the constitutive equations of the corresponding undamaged material with an adequately defined effective stress, related to the surface that effectively resists the load. In practice, the damage density function implemented in the phase-field model modifies the γ' stiffness matrix that becomes softer with the increase of damage. It was, indeed, assumed that the topological inversion is related to the softening of the γ' precipitates. Phase-field simulations were carried out from 1000 to 1200°C with an unconstrained lattice misfit and parameters that are relevant for the CMSX-4 alloy (**Figure 1**).

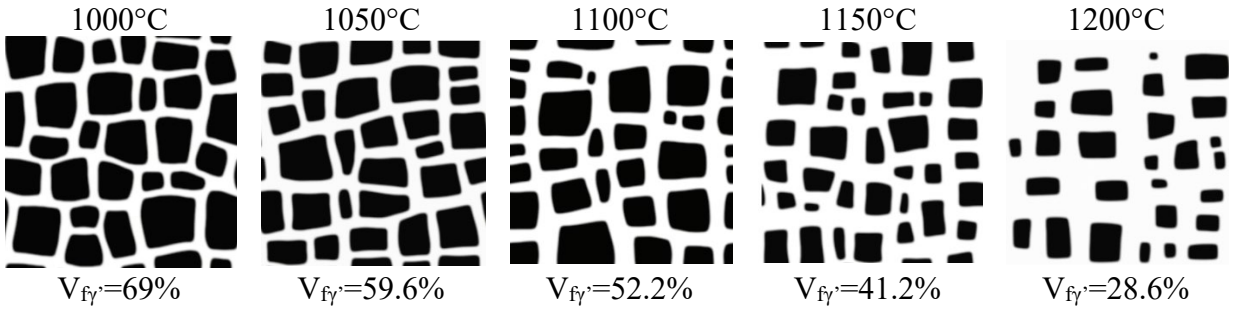

Figure 1: Cuboidal microstructures obtained by the modified phase-field model for different temperatures. The volume fraction obtained depending on the temperature is consistent with experimental observations. The γ' phase is shown in black color and γ phase in white transparency.

The results from the original phase-field model (MPF) and the creep-damage phase-field model (CDPF) are compared to show the capabilities of what was developed (**Figure 2**). For clarity of comparison, all the simulation timesteps are normalized by the rupture timestep of the corresponding creep-damage phase-field simulations (T_F). The value of T_F from each CDPF simulation is calibrated using the creep curve from a macroscopic crystal-plasticity framework with a coupled plasticity-damage formulation. The MPF calculations were continued for longer durations to see if the model was capable of predicting the loss of microstructure coherence.

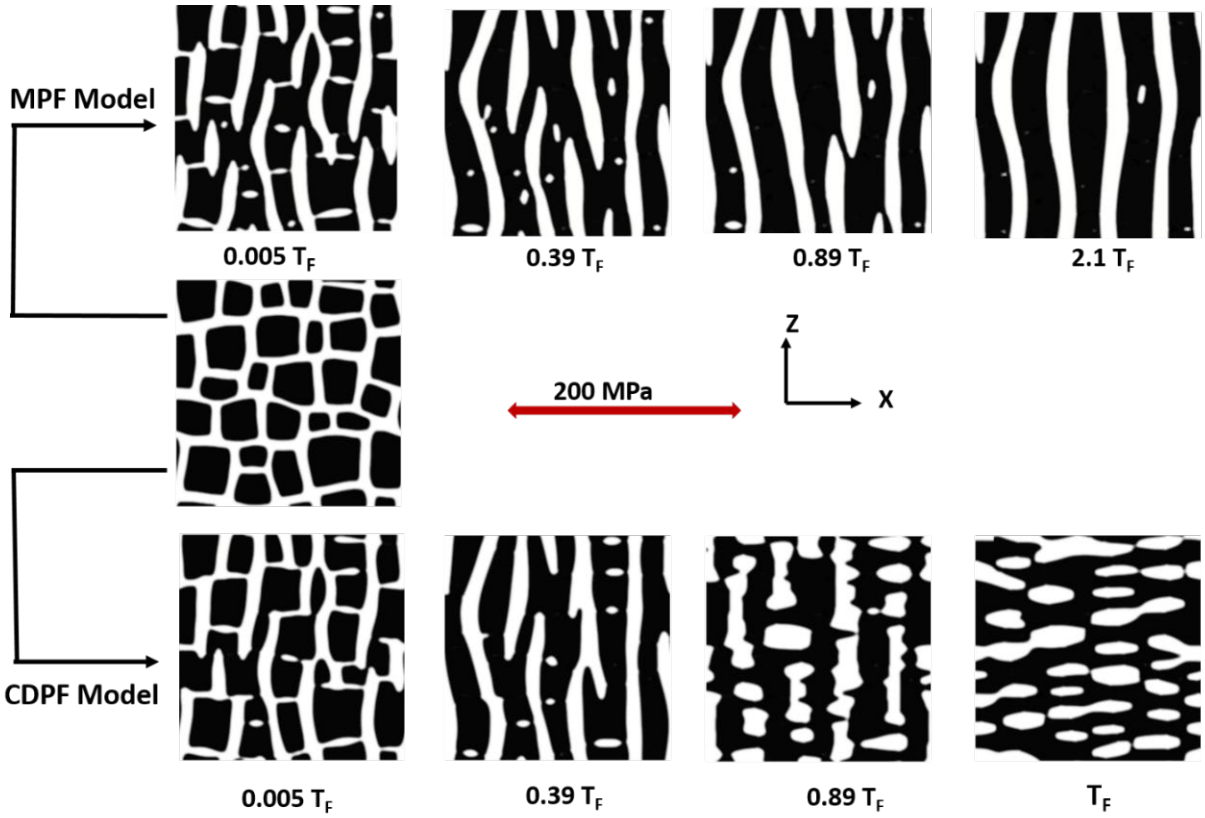

Figure 2: Comparison of simulations from The MPF model and the CDPF model at1000°C/200 MPa. The load is applied along the x-direction and TF is the time to rupture for the CDPF model.

The loss of microstructure coherence is predicted only in the CDPF simulation that shows a destabilized microstructure at the transition between the secondary and tertiary creep stages.

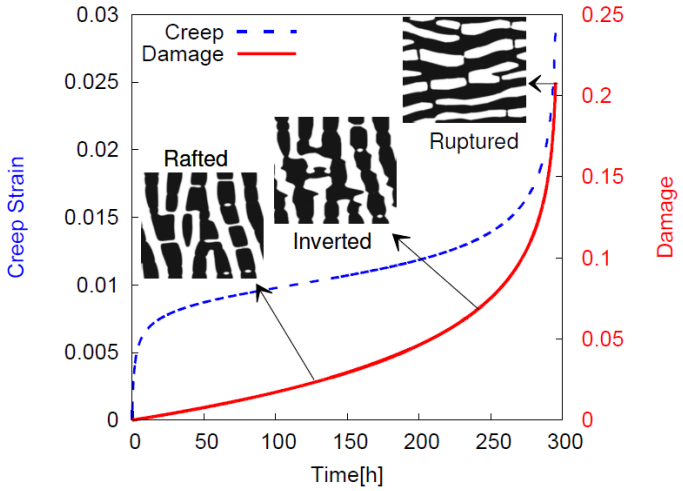

Figure 3 shows the microstructure evolution during creep in context.

Figure 3: Macroscopic crystal plasticity curves for 1050°C/150 MPa. CDPF microstructures at various points on the curves are added.

The experimental studies on the effect of volume fraction on topological inversion revealed that topological inversion only happens for superalloys with γ' volume fractions higher than 50% (see Figure 4), which is in agreement with the experimental findings in the literature.

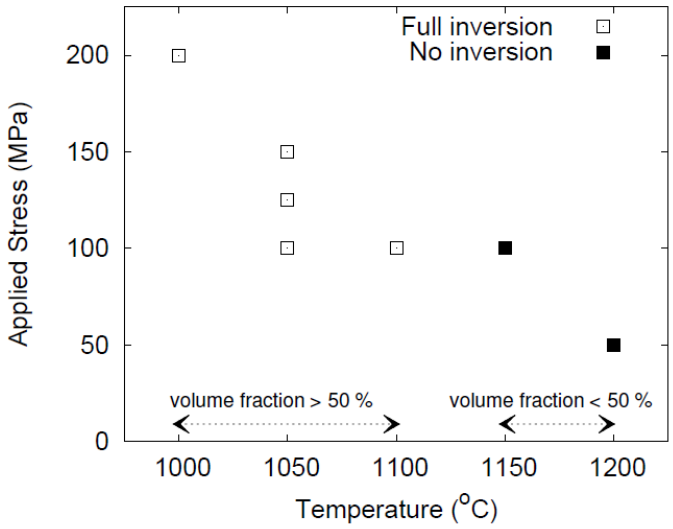

Figure 4: Summary of the conditions investigated and when topological inversion was observed.

II.2 A Phase-Field-Informed Micro-Mechanical Approach on the Effect of Lattice Misfit in Ni-based Single Crystal Superalloys

As a step towards realistic modeling and to leverage the maximum capability of two separate successful mesoscale frameworks already used for Ni-based single-crystal superalloys, namely multi-phase field model (Harikrishnan and le Graverend, 2018; Steinbach et al., 1996) and finite-element crystal plasticity (le Graverend et al., 2014b; Méric and Cailletaud, 1991), we present a bottom-up scale-bridging strategy to better understand the effect of the microstructural state on macro-scale performance of a ⟨001⟩-oriented Ni-based single-crystal superalloy. Here, instead of artificially sketching idealized microstructures for FE calculations, several realistic 3D phase-field microstructures with the right γ' volume fraction, as well as shape and distribution of the precipitates at the envisioned temperature/stress conditions, are simulated (using accurate thermodynamic descriptions and heat treatment conditions). Subsequently, the initial cuboidal and rafted microstructures are imported into an FE crystal plasticity framework. After that, the mechanical response of these 3D statistically volume elements (SVE) assigned with different materials properties for each phase is compared for a strain-controlled tensile test up to 2% strain and cyclic test with $\Delta\varepsilon = 2\%$ at a strain rate of $\dot{\varepsilon} = 10^{-3}\ s^{-1}$.

For the sake of demonstrating the effect of precipitate shape on the macroscale response, six different natural lattice misfits similar to experimental findings at high temperature were used (Van Sluytman and Pollock, 2012) to generate six differently-shaped cuboidal microstructures (Figure 5a to f): δ = -0.2%,-0.25%, -0.3%, -0.35%, -0.4%, and -0.5%. The aging conditions were simulated from explicit seeding of spherical nuclei using a quasi-random placement of nucleation sites and periodic boundary conditions that are maintained throughout the simulations. The simulation boxes are large enough to accommodate up to two orders of magnitude increase in the size of

precipitates. The different rafting stages are named based on a percentage of the primary creep stage with respect to time. For instance, 20% complete corresponds to a microstructure that was

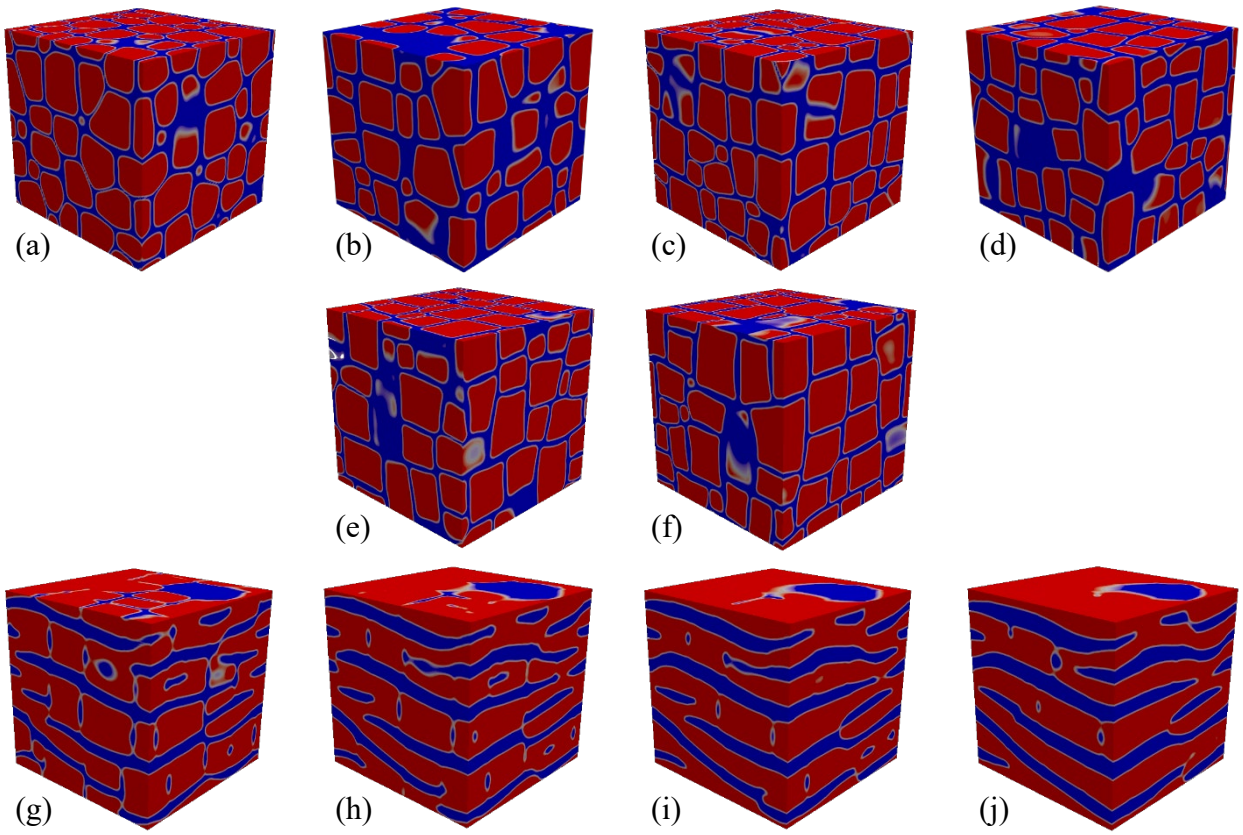

obtained at a time step that is 20% of the time step necessary to form the stabilized microstructure, namely the 100% complete.

Figure 5: Microstructures obtained by phase field simulations. Different lattice misfits: (a) -0.2%, (b) -0.25%, (c) -0.3%, (d) -0.35%, (e) -0.4%, and (f) -0.5%. Different stages of rafting: (g) 20% complete, (h) 40% complete, (i) 60% complete, and (j) 100% complete. The blue region represents the γ phase and the red one the γ' phase.

The γ-phase was considered as a continuous medium while an Eshelby tensor was employed for the γ' precipitates. The crystal-plasticity model employed was lattice-misfit dependent via an isotropic hardening variable depending on the value of the lattice misfit (unconstrained and constrained).

Figure 6a shows the simulated macroscopic stress-strain curves obtained on cuboidal microstructures having natural lattice misfits ranging from -0.2% to -0.5%. It is observed that the larger the natural lattice misfit is, the softer the mechanical response. This result is consistent with what was found in the discrete dislocation dynamics (DDD) simulations by Gao *et al.* (Gao et al., 2015).

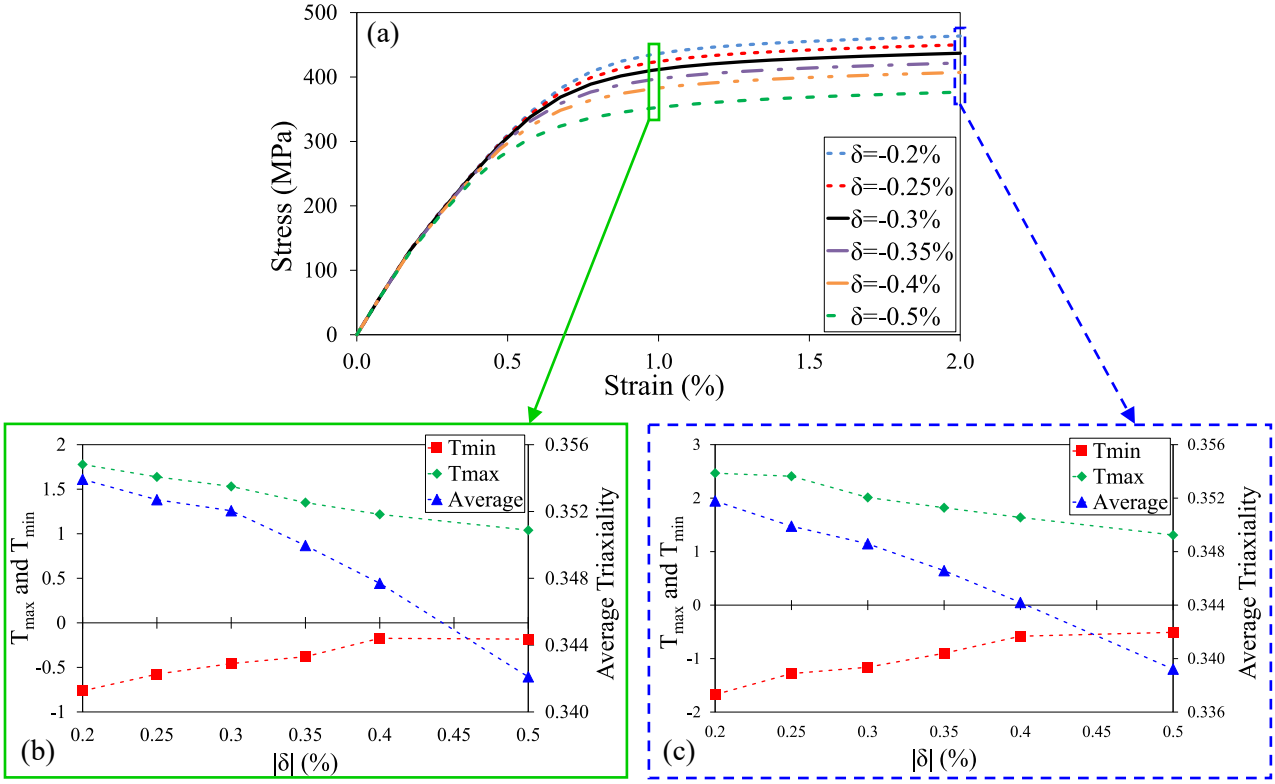

Figure 6: (a) Simulations of a monotonic tensile test at 10^{-3} s^{-1} at 1050°C up to 2% for the six natural lattice misfits investigated. At 1% (b) and at 2% (c), the maximum, the minimum and the averaged triaxiality values are provided for each natural lattice misfit.

Figure 7 shows the accumulated plastic strain distribution in the SVEs with different natural lattice misfit at 2% macroscopic total deformation, i.e., after 20 seconds. One can notice the spread of plastic deformation to the γ' phase increasing with the lattice misfit value. Simulations were also performed for different stages of rafting and highlighted that the triaxialities decrease with the percentage of rafting completion, which would mean that rafting brings more ductility. This is in contradiction with Pessah-Simonetti *et al.* (Pessah-Simonetti et al., 1993), but one should keep in mind that topologically-close packed phases are experimentally formed (Rae et al., 2000) and are not taken into account in the simulations.

Five strain-controlled cycles at 10^{-3} s^{-1} and with $\Delta\varepsilon_t = 2\%$ were simulated for six different SVE realizations having different natural lattice misfit values. It was showed that the average stress triaxiality in the volume during the five cycles depends on the natural lattice misfit value. Here, the realization with a natural lattice misfit of -0.3% produced the least average triaxiality in the volume, which is consistent with what Zhou *et al.* (Zhou et al., 2004) obtained at 1100°C on TMS alloys.

It was also pointed out that a 60% rafting developed the smallest average stress triaxiality value amongst the investigated case (the overall smallest is reached at 56% based on the trendline). It is because the 60% case is the only one for which one of the cycles develops a negative stress triaxiality, which slows down the damage process (Brünig et al., 2018). This result was consistent with experimental results obtained by Ott and Mughrabi (Ott and Mughrabi, 1999) on the effect

of microstructural states on the cyclic deformation curves of CMSX-4 and CMSX-6 at 950°C and for $\Delta\varepsilon_t = 1.2\%$.

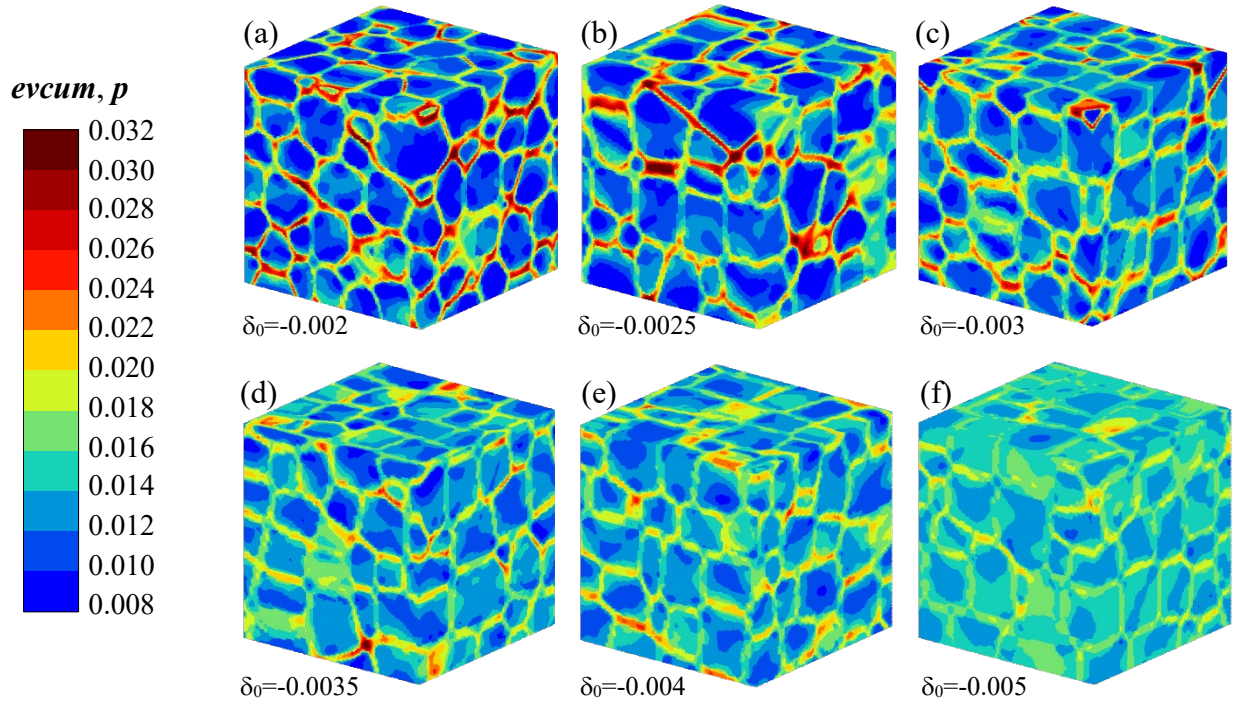

Figure 7: Accumulated plastic strain distribution at 2% total deformation after a monotonic tensile loading at 1050°C and $\dot{\varepsilon} = 10^{-3}s^{-1}$ for the six natural lattice misfits: (a) -0.2%, (b) -0.25%, (c) -0.3%, (d) 0.35%, (e) -0.4%, and (f) -0.5%.

II.3 MODELING THE ROLE OF OXIDATION ON CREEP LIFETIME

High-temperature components in jet and turbo engines are exposed to harsh corrosive environments that are detrimental and modify the mechanical behavior and lifetime. Indeed, oxidation comes with a depleted zone (Akhtar et al., 2005; Dryepondt et al., 2005), vacancies injection, and acceleration of diffusion processes while forming an oxide scale. The growth of fast-growing cationic-type oxides during the interdiffusion enables a continuous injection of vacancies due to interfacial reactions. The vacancies in excess may be reinjected into the material and, therefore, alter the mechanical behavior either by producing deformation pores or by coarsening with already existing pores, namely solidification and homogenization pores (Deacon et al., 1985; Dunnington et al., 1952; Engell and Wever, 1957). So, oxidation has a permanent or ‘‘static’’ effect on creep rate with enhancing microstructure degradation, and a ‘‘dynamic’’ effect with the acceleration of dislocation motion. These two effects are coupled and lead to higher creep rates and shorter times to rupture.

A crystal plasticity framework already described in (le Graverend, 2019; le Graverend et al., 2014b) was employed. The model follows a micro-macro approach. The developed function allows accounting for the coupling between surface roughness, which depends on the amount of plasticity, and oxidation kinetics. A Lorentzian function was found to better depict what was experimentally obtained by Pei *et al.* (Pei et al., 2018) who showed the correlation between surface

roughness and oxidation kinetics. The effect of plasticity on the oxide thickness was demonstrated by Reuchet et al. (Reuchet and Remy, 1983) who showed that the higher the stress amplitude during mechanical cycling, the thicker is the oxide scale at 900°C

Figure 8 highlights that the simulated oxidation kinetics is similarly affected by the surface roughness to what was obtained by Pei et al. Having higher mass gain or oxide thickness for higher temperatures is consistent with what was obtained by Hussain et al. (Hussain et al., 1995). The magnitude of e_{ox} is compatible with the magnitude found by Bensch et al. (Bensch et al., 2012) for the Renee N5 at 980°C.

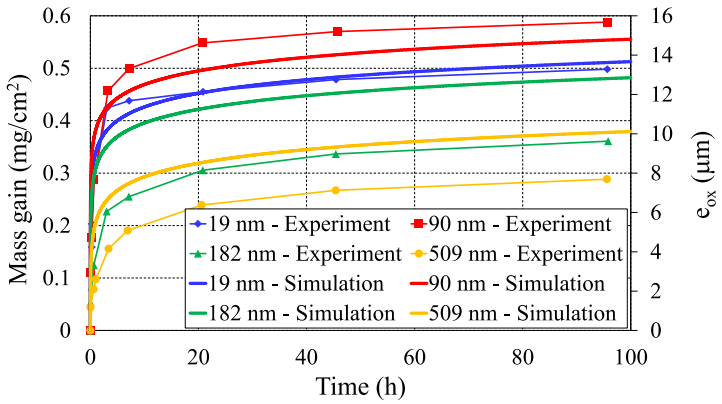

Figure 9: Comparison between the evolution of the mass gain obtained by Pei et al. at 1000°C for a Ni-4.0Cr-5.7Al single crystal superalloy for different surface roughnesses, namely 19, 90, 182, and 509 nm, and the evolutions of the oxide thickness at 1150°C and predicted by the model presented in the previous section.

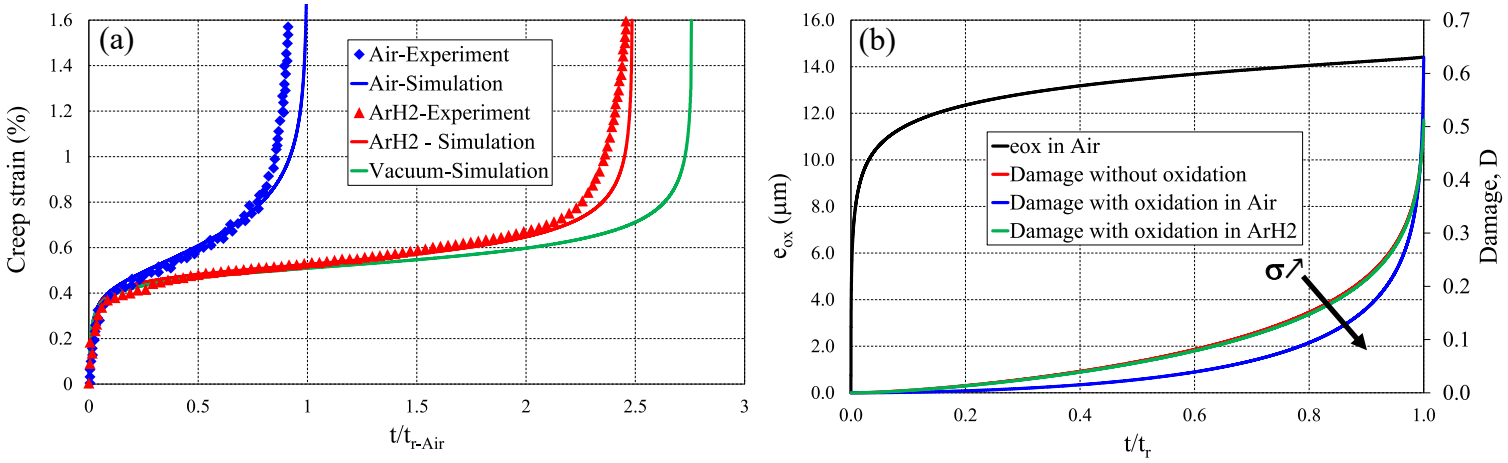

Figure 8: (a) Comparison between the experimental results in air and in ArH2 and the simulations performed with the model presented in the previous section. The curves are normalized by the time to rupture in air. The experimental results are adapted from Dryepondt et al.. (b) Evolution of e_{ox} and the damage density function D with and without oxidation. t_r is the time to rupture for the simulation considered.

The increase of the plastic strain rate in the secondary creep stage is perfectly reproduced by the model without modifying the amplitude of the primary creep stage (Figure 9a). The oxidation for the hydrogenated argon (ArH2) environment was obtained by considering what Dryepondt et al. (Dryepondt et al., 2005) got by TGA analyses under hydrogenated argon (ArH2) and synthetic

air at 1150°C. The model predicts a longer lifetime than the experimental result for ArH2. It is because the oxide thickness is smaller leading to less softening of the mechanical behavior and, therefore, to a longer lifetime. The curve for a creep test at 1150°C/80 MPa in vacuum was also added to show the maximum reachable lifetime predicted by simulation. Figure 9b shows how evolves e_{ox} as well as the damage density function with and without oxidation. Oxidation acts as if a higher stress was applied which increases the non-linearity of the damage evolution. It is consistent with the physics of oxidation that creates a depleted zone and, therefore, decreases the cross-section area leading to higher effective stresses, as predicted by the Continuum Damage Mechanics.

The effect of plastic deformation on the oxidation kinetics was also investigated by considering four pre-plastic deformations on the mechanical behavior and lifetime during creep tests at 1150°C/80 MPa. As expected, pre-deformations led to shorter lifetime during creep, as shown in (Ayrault, 1989; Nathal and Mackay, 1987). Thus, the effect of plasticity on oxidation kinetics is qualitatively consistent with previous experimental results.

II.4 DAMAGE DENSITY FUNCTION FOR NON-ISOTHERMAL LOADING

Damage prediction has always been a subject of great importance for the accurate and realistic modeling of inelastic deformation and failure behavior of engineering materials. It is why many damage models have been already proposed to analyze the fracture behavior of metals (Needleman and Tvergaard, 1984; Stoughton and Yoon, 2011; Tvergaard, 1982; Wierzbicki et al., 2005). Two main approaches can be distinguished. The first one is a micromechanics-based damage model that was originally proposed by Gurson (Gurson, 1975). The other approach to damage analysis is Continuum Damage Mechanics (CDM). CDM was initially developed in (Kachanov, 1958; Rice and Tracey, 1969). Prime examples of the CDM limitations are: the improvement of the creep lifetime at 1050°C when a unique thermal jump from 1050°C to 1200°C for 30s is introduced (le Graverend et al., 2014a), longer thermal jumps lead to longer lifetimes (Cormier et al., 2007, 2008), and cyclically cooling specimens leads to increase the plastic strain rate and to shorten the lifetime (Raffaitin et al., 2007; Viguier et al., 2011). These counter-intuitive results can not be predicted by the usual constitutive and continuum damage models that fail to consider transient behaviors and are based on hotter is shorter.

The hereby-developed phenomenological model acknowledges the role played by the microstructure in the damage evolutions by using microstructure-sensitive hardening variables. It still uses an effective stress concept (the load-carrying capacity is decreased by the degraded microstructure, i.e., the microstructure that does not have the same initial mechanical property anymore). The coupling of damage and inelastic deformation has been extensively done already for macro- (Lemaitre, 1985; Roy Chowdhury and Roy, 2018; Voyiadjis and Park, 1999) and micro-scale models (Ekh et al., 2004; Potirniche et al., 2007; Zghal et al., 2016). However, a few have been done for non-isothermal conditions (Cormier and Cailletaud, 2010; Egner, 2012) and only recently Mattiello et al. (Mattiello et al., 2018) have proposed a rate-sensitive threshold for the damage process to occur in a microstructure-sensitive framework.

The developed damage model was implemented in the PI's viscoplastic microstructure-sensitive phenomenological model written in a crystal plasticity framework (le Graverend et al., 2014b). The presented damage model was validated with isothermal/non-isothermal uniaxial/multiaxial monotonic/cyclic experiments performed on a first-generation Ni-based single crystal superalloy that shows a strong anisotropic and non-linear mechanical behavior. The

developed damage density function was also implemented in an anisotropic damage formulation. As shown in Figure 10, the developed damage model can also predict the lifetime scattering of creep tests depending on the initial volume fraction of pores F_{v0}.

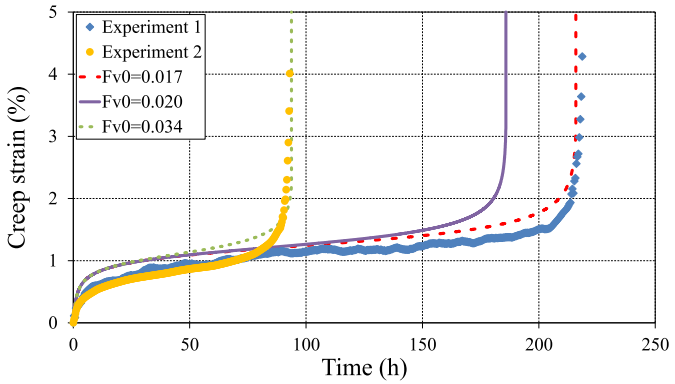

Figure 10: Simulations showing the sensitivity of the new model to the initial volume fraction of voids provided by the parameter *Fv0*.

It can be noticed that there is a non-linear accumulation of damage with the new damage parameter (see Figure 11*)*: the higher the stress is, the more abrupt the damage evolution is (Chaboche, 1978). Contrary to a Rabotnov-Kacahnov model, the non-linear accumulation is intrinsically taken into account and does not require extra functions or calibrations, as Chaboche did (Chaboche, 1974).

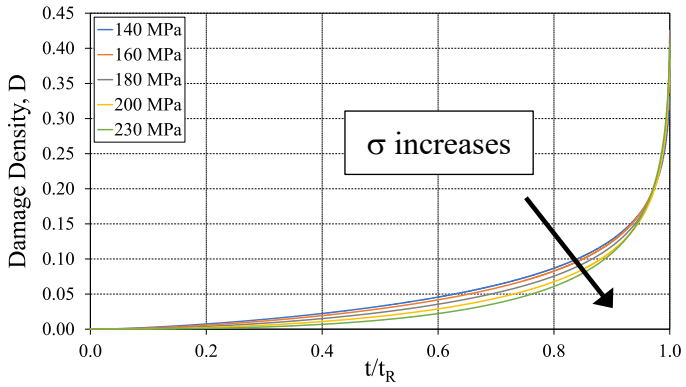

Figure 11: Evolution of the new damage variable D as a function of the time fraction t/t_R at 1050°C for the simulated curves. t_R is the simulated time at rupture.

Clearly, the new formulation better describes what is happening when a thermal jump from 1050 to 1200°C is introduced in the creep life (see Figure 12). For instance, the Rabotnov-Kachanov model predicts a failure during the thermal jump in Figure 12b and c, contrary to the new formulation. Despite a steep improvement brought by the new model, the residual lifetime is still smaller for a 90s thermal jump compared to a 30s thermal jump while the opposite was shown in (Cormier et al., 2007), the 90s thermal jump experimentally leads to a very large strain jump that is not described by the model (Figure 12b), and the plastic strain rate is increased subsequently to a thermal jump while it was shown that it is not always the case (le Graverend et al., 2014a). This last goes against what is known about when a particle is sheared or by-passed (Mohles et al., 1999) and is not correctly understood for now.

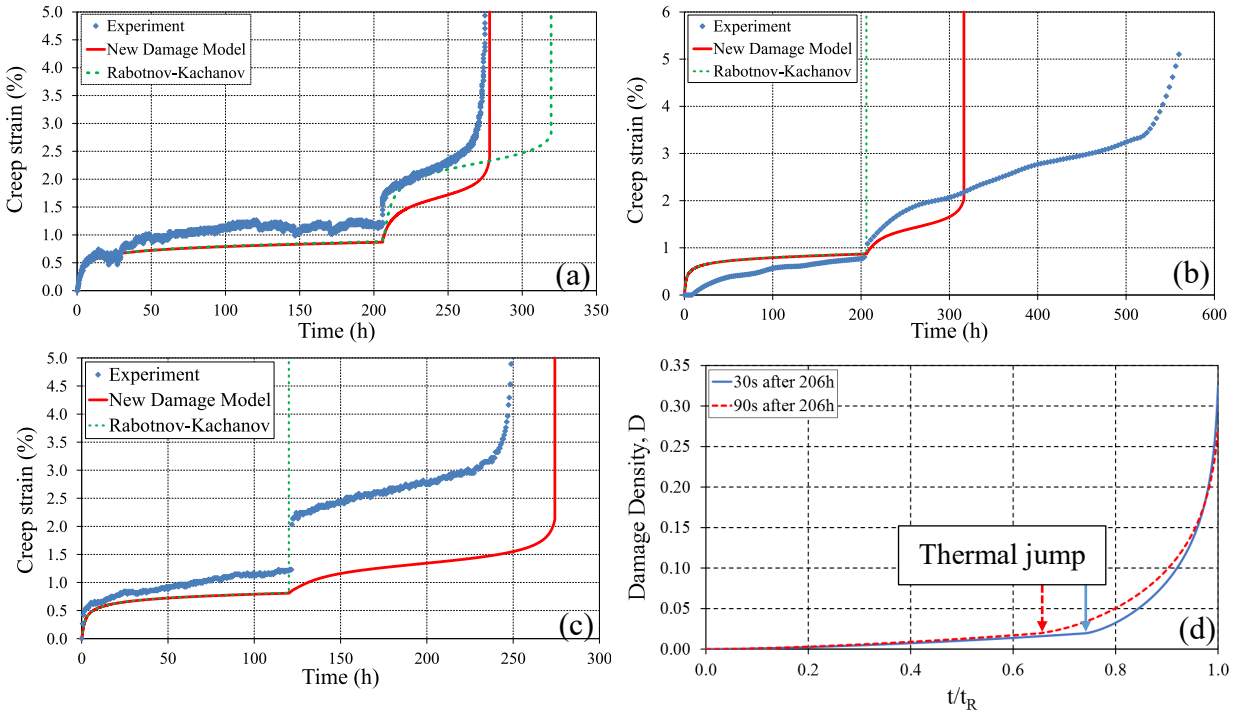

Figure 12: Creep tests at 1050°C/140 MPa for which a thermal jump of (a) 30s and (b) 90s has been introduced after 206h of testing. In (c), the 90s thermal jump has been introduced after 120h. (d) is the evolution of the damage density function for the simulated curves in (a) and (b).

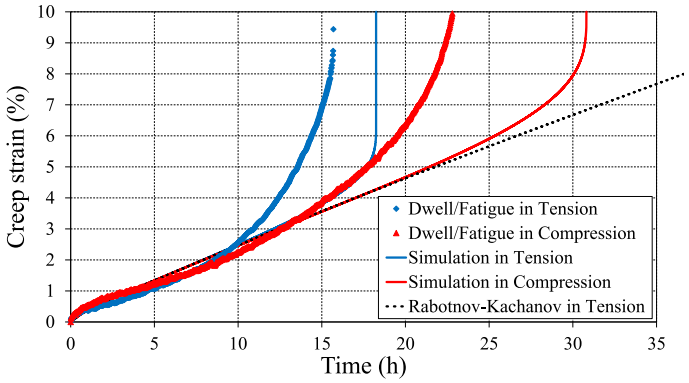

Figure 13: Simulation of a tension dwell/fatigue test (blue diamond) and a compression dwell/fatigue test (red triangle). The "New Damage Model" has been used for simulating the two tests (red and blue lines) while the "Rabotnov-Kachanov" model has only been used for simulating the dwell/fatigue test in tension

Contrary to the Rabotnov-Kachanov model, the new model can predict the lifetime of fatigue loading. **Figure 13** exhibits that the new damage model respectively predicts a failure after 16.6h and 29.3h in tension and compression, whereas the experimental specimens failed after 15.7h and 22.8h. The Rabotnov-Kachanov model does not predict a failure even after 50h in tension because it does not accumulate damage in compression, contrary to the present damage model. One can argue that the simulated shapes of the curves are not consistent with the experimental ones. The

damage model cannot be taken responsible for it, the flow rule can. Despite a not-perfect prediction of the mechanical behavior in dwell/fatigue, the difference in terms of lifetime between tension and compression as well as the final predicted lifetimes are in good agreement.

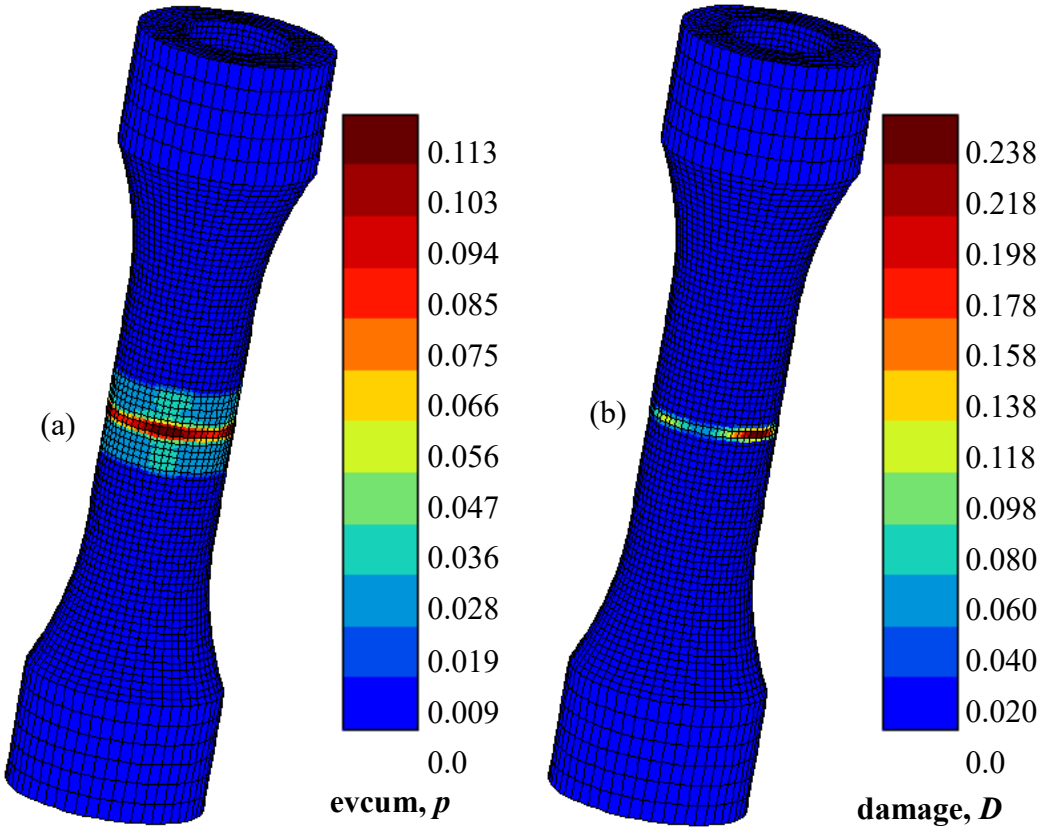

Figure 14: (a) Accumulated plastic strain and (b) damage distribution at rupture ($N_{f\text{-}predicted}$=855) for a tube subjected to tension/torsion at 1050°C/σ_{Mises}=113 MPa.

A FE simulation has been performed for tension/torsion at 113 MPa with the anisotropic damage that gave a lifetime of 855 cycles which have to be compared to the experimental one of 706 cycles (see Figure 14). Even if the simulation overestimates the number of cycles to failure, the lifetime is shorter than the pure torsional case having a higher von Mises stress applied. Therefore, as already mentioned, the current damage formulation which utilizes the kinetics of the hardening variables takes well into account the strong interactions between loading types.

II.5 Effect of multiaxiality on microstructure evolution and lifetime

A vast majority of the engineering components used for high-temperature applications contain cut sections, holes, notches, and cooling channels. These geometrical features create regions of stress concentrations and multiaxial stresses, making the durability of these components most critical. Therefore, the microstructural instability associated with these regions needs to be well-understood before coming up with complex damage models and life predictions of Ni-based single crystal superalloys. Conducting a uniform state of triaxial stress requires a complex experimental setup. However, this problem could also be tackled through straightforward laboratory experiments by

axial tensile loading on circumferentially notched specimens (Hayhurst and Felce, 1986). The notch promotes stress concentration and changes the stress state from uniaxial to multiaxial (Lukáš et al., 2001b). Further, by varying notch geometries, different multiaxial stress states were carefully investigated. Previous studies in the literature suggest that a notch could either have a weakening or a strengthening effect depending on the notch geometry and loading conditions. Studies on multiaxial creep deformation of single crystal superalloys previously demonstrated an order of magnitude increase in the lifetime of single crystal superalloys, but at an intermediate temperature and high stresses (Basoalto et al., 2000). However, creep testing at very low temperatures and very high stresses reduces the effect of notch sensitivity. Therefore, three triaxialities for four different stress conditions (160 MPa, 180 MPa, 200 MPa, 230 MPa) at 1050°C were investigated. Previous multiaxial experimental studies utilized double-notch Bridgman creep specimens (Basoalto et al., 2000; Cao et al., 2020). The advantage of such a design is that one of the notches that is still intact after the creep rupture can be utilized for better microstructural characterizations at failure. However, the two notches should sufficiently be apart to avoid stress field interference and it is also not economically viable. Using the Bridgman's criterion, three triaxialities, viz. 0.5, 0.84, and 1.0, were designed. As there is a heterogeneous strain distribution at different parts of the specimen similar to what was documented in (Cao et al., 2020), total engineering strain ($\Delta L/L_0$) of the specimens was plotted against the elapsed time. Here, L_0 is the original gauge length of the specimen. All the experiments were performed on ⟨001⟩-oriented specimens.

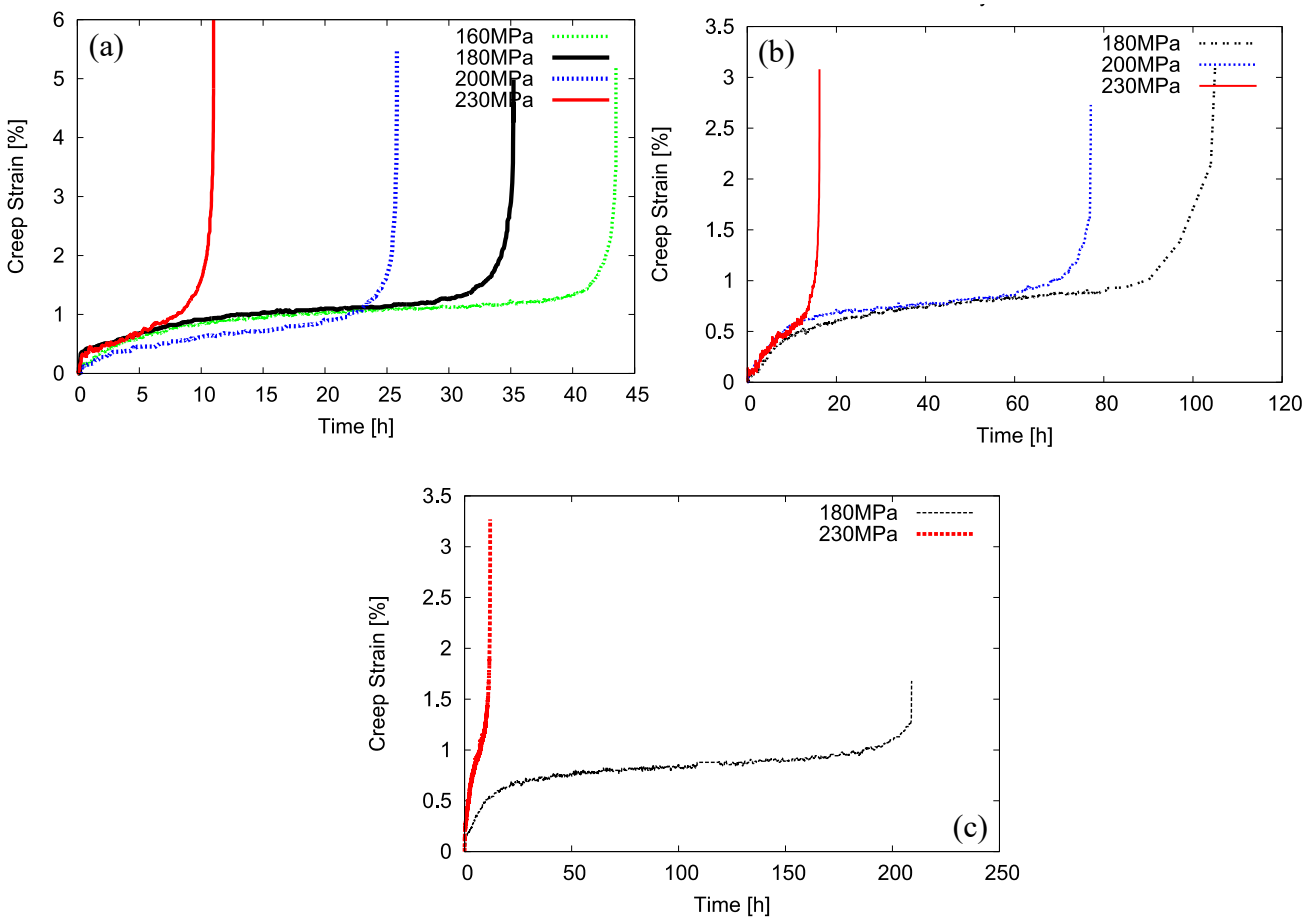

Figure 15: Comparison of the different stress investigated at 1050°C for T= (a) 0.5, (b) 0.84, and (c) 1.

A significant notch-strengthening effect can be observed in the creep data obtained from a triaxiality of 0.84 (see Figure 15b and Table 1 to compare the creep lifetime and rupture strains). Immediately after loading, an elastic/plastic stress distribution is established; as time progresses, the creep and damage formation cause stress redistribution in the notch (Hayhurst and Felce, 1986). Alternatively, in other words, the stress and rate of deformation are the highest initially and relax over time as a steady-state is reached. Simultaneously, the plastically deformed regions in the notch root get constrained by an elastic core due to which the strain-controlled creep relaxation phenomenon dominates the subsequent plastic flow (Law and Blackburn, 1980). In polycrystal alloys, it was found that the increased strain rates during tertiary creep will cause the axial stresses to redistribute (Hayhurst et al., 1978). However, this could not be true in the case of steep tertiary creep observed in MC2 superalloys and could explain why there was no notch-strengthening effect in the case of $1050°C/230 MPa for specimens with triaxiality 1. According to Hayhurst et al. (Hayhurst et al., 1978), magnitudes of the effective stresses and the magnitude of the multi-axial stress-state that causes damage determines the degree of stress redistribution. Therefore, the magnitude of rupture strain depends on the degree of stress redistribution that is governed by the sensitivity of the notch.

The notch-strengthening may be due to the constraint effect of the notch where some regions in the creeping notched specimen constrain each other leading to stress redistribution (Lukáš et al., 2001a). However, it is interesting to note that, among all the specimens tested at 1050°C/230 MPa, there is a notch strengthening for the specimen with triaxiality 0.84 and a notch weakening for the triaxialities 0.5 and 1. However, for a lower stress condition (1050°C/180 MPa), a notch-strengthening effect was observed for both specimens with triaxialities 0.84 and 1.0 (see Figure 15b and c). This comparison also sheds light on the sensitivity of the loading conditions for the notch strengthening/weakening effect. This can be further explained only by post-mortem EBSD analysis of the specimens to gauge the effect of lattice rotations on the creep damage in the notched specimens.

Table 1: Experimental uniaxial and multiaxial creep data for the investigated conditions. Time to rupture is denoted as t_r.

	T=0.3 (Uniaxial)		T=0.5		T=0.84		T=1	
Conditions	t_r	rupture	t_r	rupture	t_r	rupture	t_r	rupture
(°C/MPa)	(h)	ε(%)	(h)	ε(%)	(h)	ε(%)	(h)	ε(%)
1050/230	15.4	15.8	11.0	6.0	16.2	3.2	11.9	3.3
1050/200	43.9	10.9	25.8	5.5	77.1	2.7	66.4	3.4
1050/180	63.3	7.5	35.2	5.0	105	3.1	209.0	1.7
1050/160	143.1	6.0	43.5	5.2	269.5	3.3		

Crystal-plasticity simulations were carried out with the damage density function developed in (le Graverend, 2019). Figure 17 shows the results for 180 MPa. What was found experimentally, namely that there is a notch weakening for T=0.5, is not numerically obtained. In addition, the simulations predict that the longest lifetime should occur for T=0.84, which was not obtained at 180 MPa but at 200 and 230 MPa. Even if the simulations predict that a cylindrical notch improves the lifetime, as obtained experimentally, it overestimates the lifetime too much. It can be attributed is to the pseudo-cubic slip systems that were neglected.

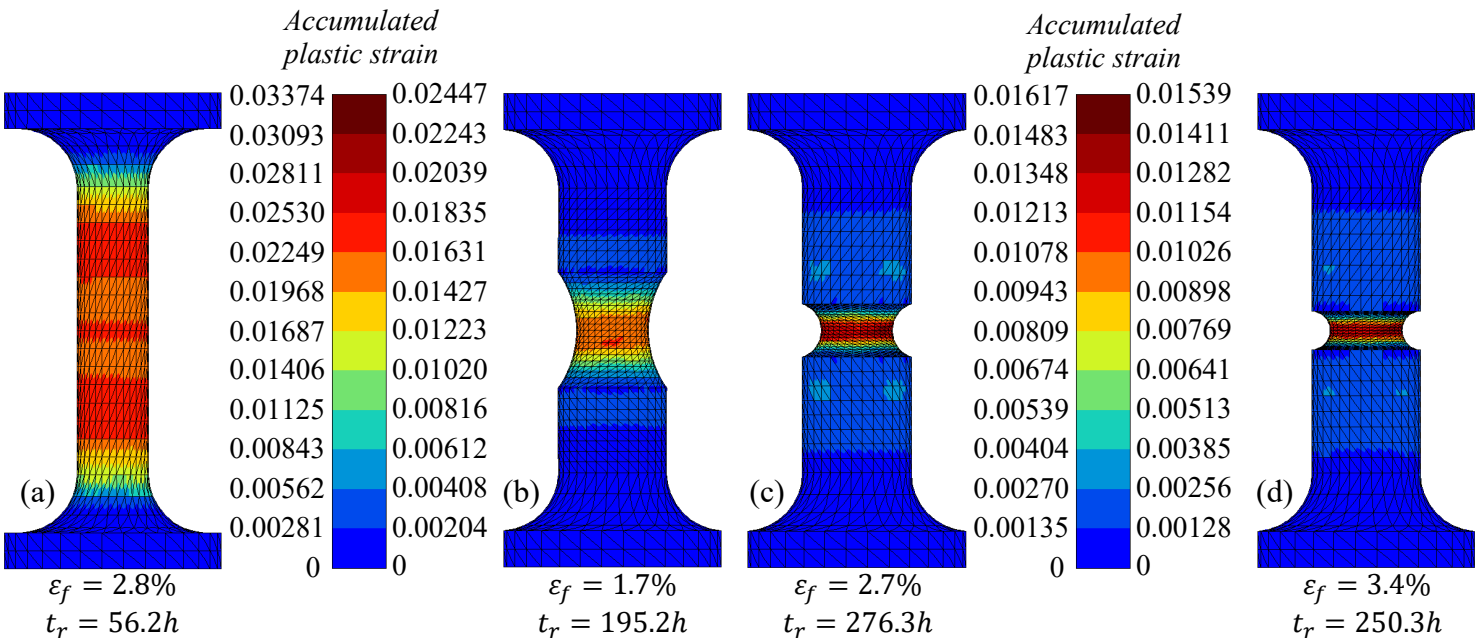

Figure 16: Accumulated plastic strain distribution at rupture for a creep test at 1050°C/180MPa: (a) uniaxial, (b) T=0.5, (c) T=0.84, and (d) T=1.

II.6 CRYSTALLOGRAPHY-DEPENDENT PHASE-FIELD MODEL AND EVALUATION OF PERFORMANCE

Controlling the single crystal orientation in a low modulus ⟨001⟩ direction and maintaining it parallel to the centrifugally loaded blade axis also minimizes the thermal stresses and improves the thermal fatigue resistance (Ardakani et al., 1999). However, in reality, the intricate internal cooling channels and the strain grain formation near the single-crystal seed region (Yang et al., 2005) result in casting inaccuracies leading to slight deviations from perfect [001]-orientations (Li et al., 2008). Furthermore, attaining a perfect parallel alignment of the blade axis with the centrifugal load is not always practically possible (Matan et al., 1999a). Even though misorientations up to 15° for certain applications (Mattiello, 2018) are within the permissible level, since each blade has a varying degree of misorientation, the mismatch between loading and crystallographic axes leads to a significant scatter in properties resulting in a mistuned-bladed assembly inside the aircraft engine (Rajasekharan and Petrov, 2019; Rajasekharan and Petrov, 2018).

At the microstructural level, the pattern and orientation of γ' precipitates in the cuboidal state are different for each crystallographic orientation. In ⟨001⟩ -oriented specimens, depending on the sign of natural lattice misfit and applied stress, the rafts are formed either perpendicular (negative misfit/positive stress and positive misfit/negative stress) or parallel (negative misfit/negative stress and positive misfit/positive stress) to the loading axis (Pollock and Argon, 1994). However, the orientation of precipitates and directional coarsening is at 45° to the applied stress axis in ⟨011⟩ as compared to ⟨001⟩ (Gaubert et al., 2015). The platelet-like rafts in ⟨001⟩, the 45° rod-like rafts (Gaubert et al., 2015; Sass and Feller-Kniepmeier, 1998) in ⟨011⟩, and the irregular rafts (Caron et al., 1988; Desmorat et al., 2017) in ⟨111⟩ suggests the sensitivity of microstructure evolution to crystallographic orientations. Despite knowing that different orientations have different types of

rafting in Ni-based single-crystal superalloys, not many studies were dedicated to understanding the sensitivity of microstructural evolution due to variation in crystallographic orientations (Ardakani et al., 1998; Sass and Feller-Kniepmeier, 1998). Therefore, the objective of this study was to understand the microstructural gradients associated with the change in the orientation and quantify their direct effect on the mechanical performance.

In this work, for the first time, a crystallographic-sensitive phase-field method was developed to study the effect of crystalline orientations on the evolution of γ' precipitate and γ channel morphology during aging and high-temperature/low-stress tensile creep. The study using realistic 3D phase-field simulations delved into elucidating the microstructural evolution and their stability depending on the crystallographic orientation.

The employed phase-field framework was the same as in (Harikrishnan and le Graverend, 2018; le Graverend and Harikrishnan, 2019, 2021). However, a 3D rotation matrix (R) depending on the three Euler angles was introduced. Once the Euler angles were known for a particular orientation, the corresponding rotation matrix was used to rotate the stiffness and Eigen strain matrices. Here, only the three crystallographic orientations at the corner of a stereographic triangle, i.e., ⟨001⟩, ⟨011⟩ and ⟨111⟩ were considered. The figure below Figure 17 shows the initial microstructural state of those three orientations at 1050°C and for a natural lattice misfit of -0.003.

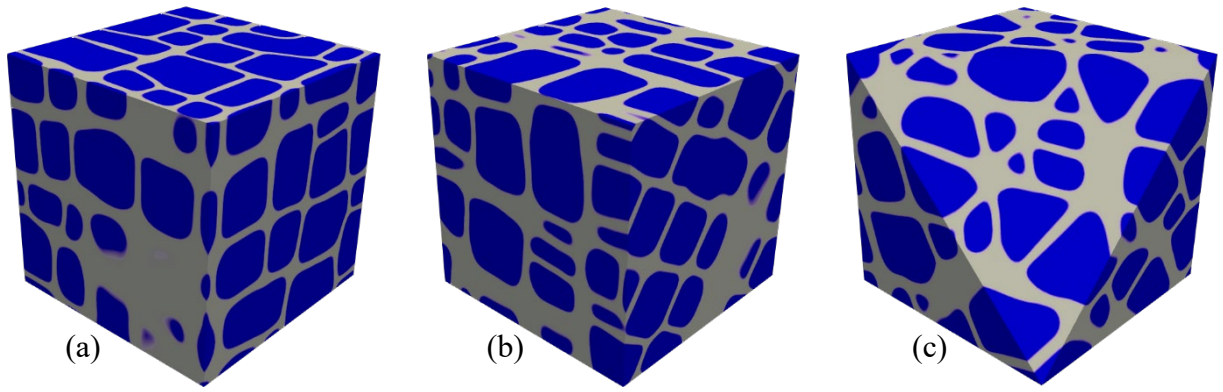

Figure 17: Phase-field simulations to form (a) ⟨001⟩-, (b) ⟨011⟩-, and (c) ⟨111⟩-oriented cuboidal microstructures at 1050°C and for a natural lattice misfit of -0.003.

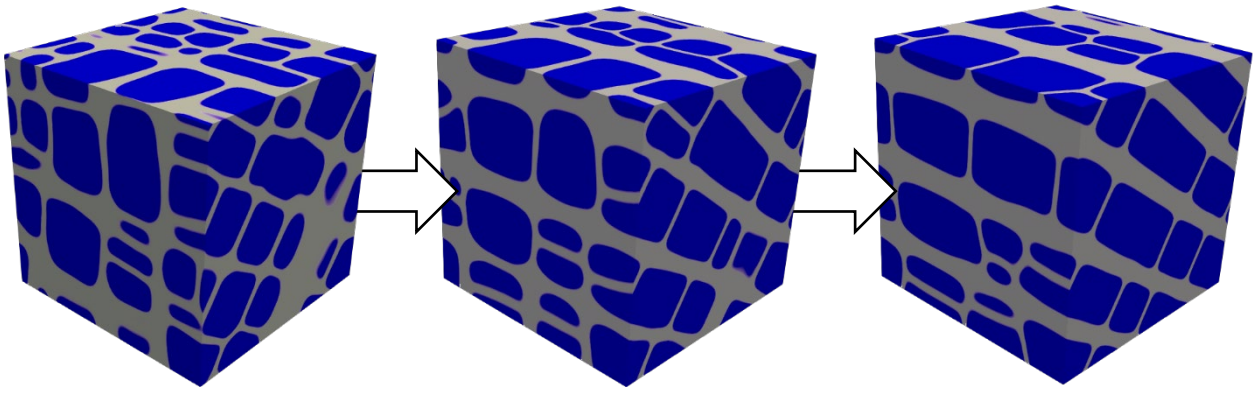

Figure 18: Phase-field simulation of a creep test at 1050°C/180 MPa on the ⟨011⟩-oriented RVE presented in the previous figure.

Figure 18 shows the evolution of the γ' precipitates when the ⟨011⟩-oriented SVE is subjected to 180 MPa. In a similar fashion as what happens when a ⟨001⟩-oriented SVE is deformed, there is a directional coarsening of the γ' precipitates along 45° planes, which is consistent with the literature.

To compare the effects of different crystallographic orientations on the macroscale performance, 3D phase-field microstructural configurations were exported as statistical volume elements (SVE) into a finite-element (FE) crystal plasticity model. Strain-controlled tensile tests up to 2% total strain at a strain rate of $\dot{\varepsilon} = 10^{-3}\ s^{-1}$ were carried out in the 3D phase-field SVEs having cuboidal and rafted states with different crystallographic orientations. Figure 19 shows the results of the monotonic tensile simulations as a function of the crystallographic orientation and the microstructural states

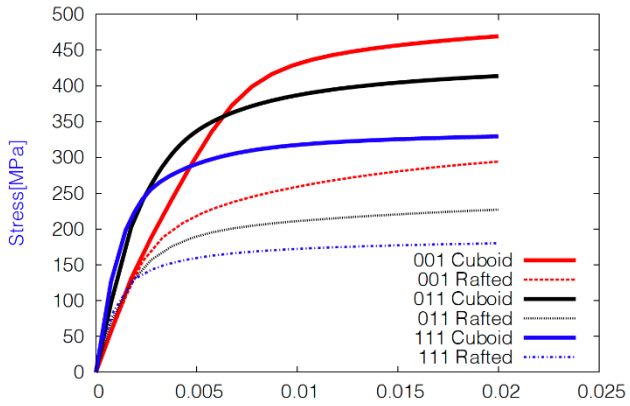

Figure 19: Crystal-plasticity finite-element simulations of a monotonic tensile tests at 10^{-3} s^{-1} 1050°C for different orientations and microstructural states.

II.7 PHASE-FIELD-INFORMED VECTORIAL MODELING OF RAFTING IN NI-BASED SINGLE CRYSTAL SUPERALLOYS

The directional coarsening of the γ' phase, also known as rafting, cannot be avoided above 850°C. The rafting kinetics has been experimentally investigated (Epishin et al., 2000; Matan et al., 1999b; Véron and Bastie, 1997; Zhang et al., 2019) and numerically studied either with phase-field (Boussinot et al., 2009; Cottura et al., 2012; Gaubert et al., 2010) or constitutive (Cormier and Cailletaud, 2010; Desmorat et al., 2017; Fedelich et al., 2012; le Graverend et al., 2014b; Svoboda and Lukas, 1998; Tinga et al., 2009) modeling. However, the vast majority of the constitutive models accounting for rafting on the mechanical behavior only introduce a scalar parameter to describe the width of the γ channels, except Tinga et al. (Tinga et al., 2009) who introduced a vector and by Desmorat et al. (Desmorat et al., 2017) who introduced a tensor. Even if Desmorat's model is based on a thermodynamic framework and is able to overall predict the evolution of the γ channels in the three directions and for different crystallographic orientation, the model is restrained to negative lattice misfit and some results do not seem physical, such as piecewise evolutions without any saturations.

Using a scalar makes the modeling restricted to the ⟨001⟩ orientation and to uniaxial loading. However, blades are rarely perfectly ⟨001⟩ oriented (Mattiello, 2018) which leads to mechanical response scattering (Rajasekharan and Petrov, 2018), are subjected to multiaxial loading, and can experience lattice rotations (Ardakani et al., 1998; Ghighi et al., 2012; Ghosh et al., 1990; le

Graverend et al., 2018; MacLachlan et al., 2001). Amongst the few constitutive models that take into account the effect of rafting on the mechanical behavior, only two also consider the dissolution precipitation of the γ' phase and the occurrence of fine γ' precipitates in the γ (Cormier and Cailletaud, 2010; le Graverend et al., 2014b).

The work was, therefore, dedicated to formulating a phenomenological vectorial expression modeling the evolution of the γ channels in the three directions due to thermo-mechanical loading and for any crystallographic orientations. This formulation was built on the one developed by le Graverend et al. (le Graverend et al., 2014b). It considers octahedral and pseudo-cubic slip systems and takes into account isothermal and non-isothermal modifications of the microstructural state. However, how to calibrate such model since it is impossible to follow in situ the evolution of the γ channels even with X-ray and neutron diffractions that provide numerous information, such as the γ' volume fraction (le Graverend et al., 2012), the constrained lattice misfit (Diologent et al., 2003; Jacques et al., 2004), and the Young's modulus of both phases (Coakley et al., 2017)? It is why phase-field simulations for different stress levels and different crystallographic orientations were employed to calibrate the model.

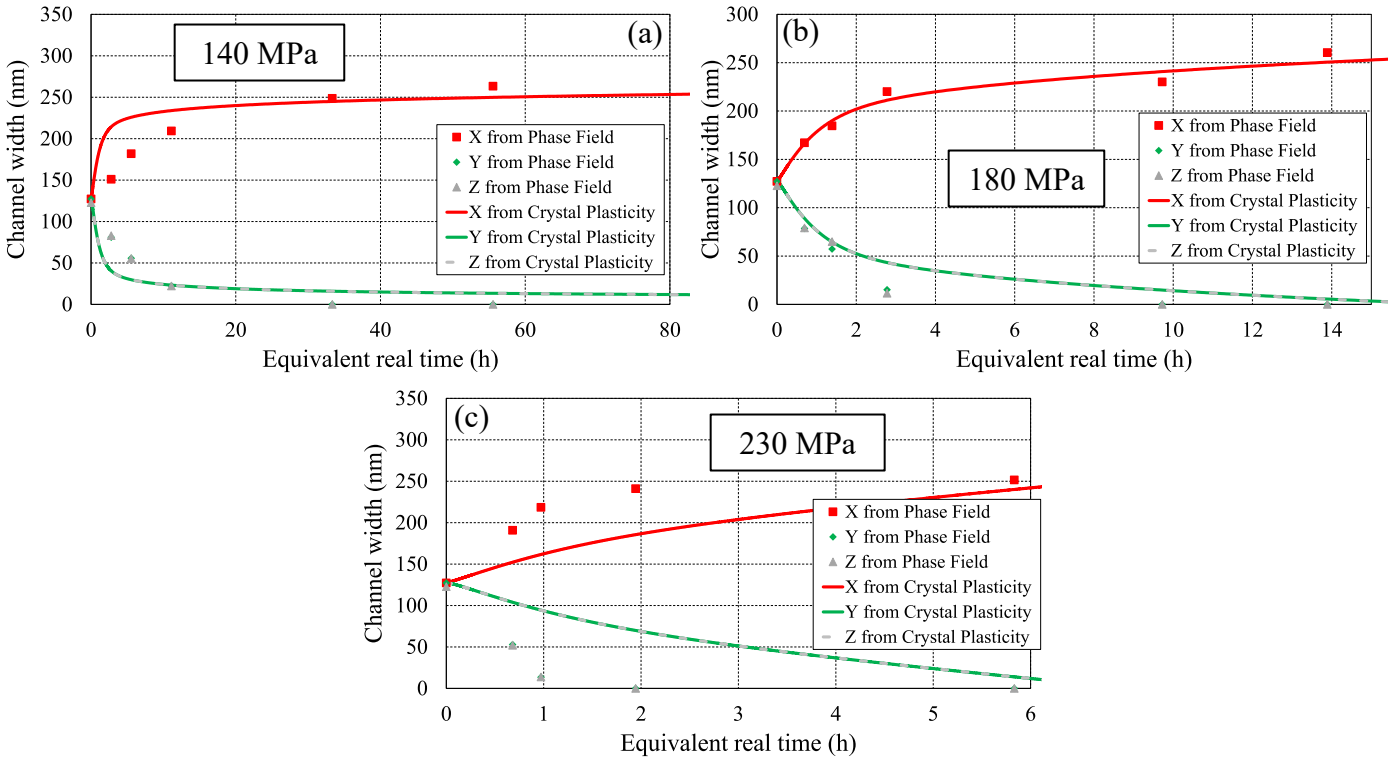

Figure 20: Evolution of the γ channel width during creep tests at 1050°C and (a) 140, (b) 180, and (c) 230 MPa applied along the x direction. The crystal-plasticity-obtained channel widths are compared with the γ channel widths obtained by phase field simulations.

Contrary to octahedral slip, the isotropic hardening for the cubic-slip systems is not Orowan dependent. Indeed, based on their mode of propagations, dislocations moving by cross-slipping should be less sensitive to the Orowan stress. Chen et al. (Chen et al., 2019) performed atomistic modeling of dislocation cross-slip in nickel. They found that cross-slip is independent of obstacle spacing for high resolved shear stress. Additionally, Sass et al. (Sass et al., 1996) found that $[\bar{1}11]$ orientation promotes a reduction of the plastic strain rate contrary to [001] and [011] that show

softening due to rafting. Therefore, it seems that the pseudo-cubic slip systems do not depend on the Orowan stress.

The 3D rafting model is sensitive to **1**) the value of the natural lattice misfit to predict N or P-type rafting, **2**) the difference in microstructure kinetics depending on the sign of the load, i.e., if the load is in tension or compression, **3**) the accumulated plastic strain (usually defined as a scalar) in each direction of the crystal or "*Natural Anisotropy Basis*", as defined by Desmorat et al. (Desmorat et al., 2017). Also, the pseudo-cubic slip systems contribute to rafting, contrary to what was done by Fedelich et al. (Fedelich et al., 2009) and Desmorat et al. (Desmorat et al., 2017). Indeed, it was shown in (Hong et al., 2011; Sugui et al., 1999) that ⟨001⟩-oriented samples with a negative lattice misfit subjected to tension display vertical γ channels with compression stresses. dislocation motion has a larger resistance so that the dislocation moves a shorter distance in a mode of cross-slip. Thus, the closing of vertical γ channels is tied to cross-slip mechanisms. Pseudo-cubic slip systems occur in near [111]-oriented specimens. These structures have been interpreted as resulting from alternating cross-slip on two octahedral planes between the opposite γ/γ' interfaces of the screw segments trailed by mobile dislocation loops (Bettge and Österle, 1999; Volkl et al., 1994). For the reasons, previously expressed, pseudo-cubic systems contribute to rafting, especially because Zhang et al. (Zhang et al., 2005) also observed cross-slip in the horizontal channels of TMS-138.

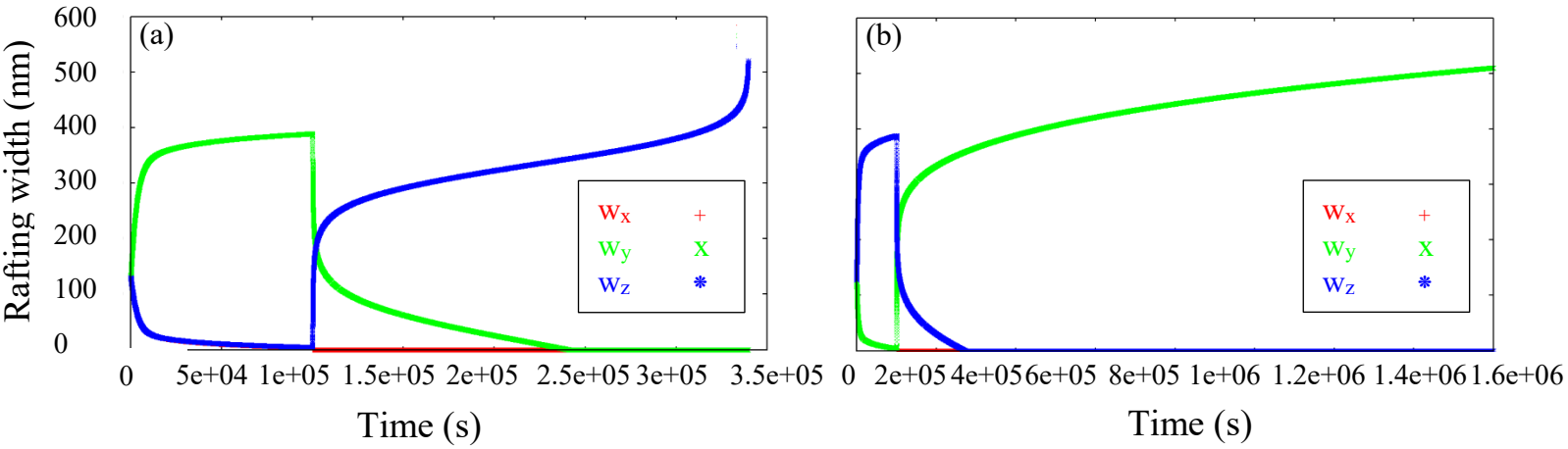

Figure 21: Simulated channel width evolutions for a creep test at 1050°C starting with a (a) compressive/(b) tension stress at -140 MPa/140 MPa along the z direction. The load is switched to a tension/compression stress at 140 MPa/-140 MPa after 100,000s. The samples are predicted to fail after 3.395e+05s and not fail even after 1,6e+6 s, respectively.

Figure 21 highlights the capacity of the model to predict microstructure evolutions even when the load is reversed. The fact that the model predicts that starting with traction leads to a longer lifetime compared to starting with compression is consistent with what was already obtained in the literature (Ayrault, 1989; Nathal and Mackay, 1987).

III. LIST OF PUBLICATIONS

CONFERENCE PAPER:

(le Graverend and Lee, 2020a)

JOURNAL ARTICLES:

(Harikrishnan and le Graverend, 2018)
(le Graverend, 2018)
(le Graverend, 2019)
(le Graverend and Harikrishnan, 2019)
(le Graverend and Lee, 2020b)
(Harikrishnan et al., 2021)
(Harikrishnan and le Graverend, 2021)
(le Graverend and Harikrishnan, 2021)
(le Graverend and (Harikrishnan, 2021)

CONFERENCE PRESENTATIONS:

1. H. Rajendran (Sp) & J.-B. le Graverend "Microstructural Damage Evolution during High-temperature Creep in Nickel-based Single Crystal Superalloys: A Phase Field Study"
   Oral presentation at the TMS 2018 conference, Phoenix (AZ), March 11-15 2018.
2. H. Rajendran (Sp) & J.-B. le Graverend "Role of Lattice Misfit in the Stability of Ni-based Single Crystal Superalloys: A Phase Field Study"
   Oral presentation at the TMS 2019 conference, San Antonio (TX), March 10-14 2019.
3. J.-B. le Graverend (Sp) & H. Rajendran "*Finite-Element Crystal Plasticity on Phase-Field Microstructures: Predicting Mechanical Response Variations in Ni-based Single Crystal Superalloys*"
   Oral presentation at the TMS 2019 conference, San Antonio (TX), March 10-14 2019.
4. J.-B. le Graverend (Sp) & R. Harikrishnan "Phase-Field-Informed Modeling of γ' Rafting in 3D during High-Temperature Creep in Ni-Based Single Crystal Superalloys"
   Euromat 2019, Stockholm, Sweden, September 1-5, 2019.
5. J.-B. le Graverend (Sp) & R. Harikrishnan "Finite-Element Crystal Plasticity on Phase-Field Microstructures: Predicting Mechanical Response Variations in Ni-based Single-Crystal Superalloys"
   Euromat 2019, Stockholm, Sweden, September 1-5, 2019.
6. H. Rajendran (Sp) & J.-B. le Graverend "*Modeling the Dependence of Microstructural Evolution on the Crystallographic Orientation in Ni-based Single Crystal Superalloys*"
   Oral presentation at the TMS 2020 conference, San Diego (TX), February 23-27 2020.
7. J.-B. le Graverend (Sp) & H. Rajendran "*Phase-field-informed Modeling of γ' Rafting in 3D during High temperature Creep in Ni-based Single Crystal Superalloys*"
   Oral presentation at the TMS 2020 conference, San Diego (TX), February 23-27 2020.
8. J.-B. le Graverend (Sp) & S. Lee "*A Damage Model with Oxidation Effects*"
   Oral presentation at the TMS 2020 conference, San Diego (TX), February 23-27 2020.
9. J.-B. le Graverend & S. Lee "*Phenomenological Modeling of the Effect of Oxidation on the Creep Response of Ni-based Single-Crystal Superalloys"*
   International Conference on Superalloys, Seven Spring, September 13-17 2020

MS THESIS AND PHD DISSERTATION

(Lee, 2019)
(Harikrishnan, 2021)

AWARD

H. Rajendran was awarded International Symposium on Superalloys Scholarship by a TMS committee.

IV. PERSONNEL SUPPORTED

Professor Jean-Briac le Graverend received summer salary support under this grant. Seugjun Lee was supported for his master's degree, and Harikrishnan Rajendran was supported for his doctoral degree.

REFERENCES

AFRL, 2014. Air Force Research Laboratory Sustainment Science and Technology Strategy. AFRL.

Akhtar, A., Hook, M.S., Reed, R.C., 2005. On the oxidation of the third-generation single-crystal superalloy CMSX-10. Metall. Mat. Trans. A 36, 3001-3017.

Ardakani, M.G., Ghosh, R.N., Brien, V., Shollock, B.A., McLean, M., 1998. Implications of dislocation micromechanisms for changes in orientation and shape of single crystal superalloys. Scripta Materialia 39, 465-472.

Ardakani, M.G., McLean, M., Shollock, B.A., 1999. Twin formation during creep in single crystals of nickel-based superalloys. Acta Materialia 47, 2593-2602.

Ayrault, D., 1989. Fluage à haute température de superalliages base nickel monocristallins. Ecole Nationale Supérieure des Mines de Paris (France).

Basoalto, H.C., Ghosh, R.N., Ardakani, M.G., Shollock, B.A., McLean, M., 2000. Multiaxial creep deformation of single crystal superalloys: modelling and validation, in: Pollock, T.M., Kissinger, R.D., Bowmann, R.R. (Eds.), International Symposium on Superalloys. TMS, Seven Springs, PA, USA, pp. 515-524.

Bensch, M., Sato, A., Warnken, N., Affeldt, E., Reed, R.C., Glatzel, U., 2012. Modelling of High Temperature Oxidation of Alumina-Forming Single-Crystal Nickel-Base Superalloys. Acta Materialia 60, 5468-5480.

Bettge, D., Österle, W., 1999. "Cube slip" in near-[111] oriented specimens of a single-crystal nickel-base superalloy. Scripta Materialia 40, 389-395.

Boussinot, G., Finel, A., Le Bouar, Y., 2009. Phase-field modeling of bimodal microstructures in nickel-based superalloys. Acta Materiala 57, 921-931.

Brünig, M., Gerke, S., Schmidt, M., 2018. Damage and failure at negative stress triaxialities: Experiments, modeling and numerical simulations. International Journal of Plasticity 102, 70-82.

Cao, L., Thome, P., Agudo Jácome, L., Somsen, C., Cailletaud, G., Eggeler, G., 2020. On the influence of crystallography on creep of circular notched single crystal superalloy specimens. Mater. Sci, Eng. A 782, 139255.

Caron, P., Ohta, Y., Nakagawa, Y.G., Khan, T., 1988. Creep deformation anisotropy in single crystal superalloys, in: Reichman, S., Duhl, D.N., Maurer, G., Antolovich, S.D., Lund, C. (Eds.), International Symposium on Superalloys. TMS, Seven Spring (PA, USA), pp. 215-224.
Chaboche, J.-L., 1974. Une loi différentielle d'endommagement de fatigue avec cumulation non linéaire. Revue Francaise de Mecanique 50-51.
Chaboche, J.L., 1978. Description thermodynamique et phenomenologique de la viscosite cyclique avec endommagement.
Chen, D., Costello, L.L., Geller, C.B., Zhu, T., McDowell, D.L., 2019. Atomistic modeling of dislocation cross-slip in nickel using free-end nudged elastic band method. Acta Materialia 168, 436-447.
Coakley, J., Lass, E.A., Ma, D., Frost, M., Seidman, D.N., Dunand, D.C., Stone, H.J., 2017. Rafting and elastoplastic deformation of superalloys studied by neutron diffraction. Scripta Materialia 134, 110-114.
Cormier, J., Cailletaud, G., 2010. Constitutive modeling of the creep behavior of single crystal superalloys under non-isothermal conditions inducing phase transformations. Mater. Sci, Eng. A 527, 6300-6312.
Cormier, J., Milhet, X., Mendez, J., 2007. Non-isothermal creep at very high temperature of the nickel-based single crystal superalloy MC2. Acta Materialia 55, 6250-6259.
Cormier, J., Milhet, X., Mendez, J., 2008. Anisothermal creep behavior at very high temperature of a Ni-based superalloy single crystal. Mat. Sci. Eng. A 483-484, 594-597.
Cottura, M., Le Bouar, Y., Finel, A., Appolaire, B., Ammar, K., Forest, S., 2012. A phase field model incorporating strain gradient viscoplasticity: Application to rafting in Ni-base superalloys. Journal of the Mechanics and Physics of Solids 60, 1243-1256.
Deacon, C., Loretto, M.H., Smallman, R.E., 1985. Behaviour of vacancies during oxidation. Materials Science and Technology 1, 344-350.
Desmorat, R., Mattiello, A., Cormier, J., 2017. A tensorial thermodynamic framework to account for the γ' rafting in nickel-based single crystal superalloys. International Journal of Plasticity 95, 43-81.
Diologent, F., Caron, P., d'Almeida, T., Jacques, A., Bastie, P., 2003. The γ/γ′ mismatch in Ni based superalloys: In situ measurements during a creep test. Nuclear Instruments and Methods in Physics Research Section B: Beam Interactions with Materials and Atoms 200, 346-351.
Dryepondt, S., Monceau, D., Crabos, F., Andrieu, E., 2005. Static and dynamic aspects of coupling between creep behavior and oxydation on MC2 single crystal superalloy at 1150 °C. Acta Materiala 53, 4199-4209.
Dunnington, B.W., Beck, F.H., Fontana, M.G., 1952. The Mechanism of Scale Formation On Iron at High Temperature. Corrosion 8, 2-12.
Egner, H., 2012. On the full coupling between thermo-plasticity and thermo-damage in thermodynamic modeling of dissipative materials. International Journal of Solids and Structures 49, 279-288.
Ekh, M., Lillbacka, R., Runesson, K., 2004. A model framework for anisotropic damage coupled to crystal (visco)plasticity. International Journal of Plasticity 20, 2143-2159.
Engell, H., Wever, F., 1957. Some basic problems of the formation and adherence of scale on iron. Acta Metallurgica 5, 695-702.
Epishin, A., Link, T., Portella, P.D., Brückner, U., 2000. Evolution of the γ/γ′ microstructure during high-temperature creep of a nickel-base superalloy. Acta Materialia 48, 4169-4177.
Fedelich, B., Epishin, A., Link, T., Klingelhöffer, H., Künecke, G., Portella, P.D., 2012. Experimental characterization and mechanical modeling of creep induced rafting in superalloys. Comp. Mat. Sci. 64, 2-6.
Fedelich, B., Künecke, G., Epishin, A.I., Link, T., Portella, P.D., 2009. Constitutive modelling of creep degradation due to rafting in single-crystalline Ni-base superalloys. Mat. Sci. Eng. A 510-511, 273-277.
Gao, S., Fivel, M., Ma, A., Hartmaier, A., 2015. Influence of misfit stresses on dislocation glide in single crystal superalloys: A three-dimensional discrete dislocation dynamics study. Journal of the Mechanics and Physics of Solids 76, 276-290.
Gaubert, A., Jouiad, M., Cormier, J., Le Bouar, Y., Ghighi, J., 2015. Three-dimensional imaging and phase-field simulations of the microstructure evolution during creep tests of <011>-oriented Ni-based superalloys. Acta Materialia 84, 237-255.

Gaubert, A., Le Bouar, Y., Finel, A., 2010. Coupling phase field and viscoplasticity to study rafting in Ni-based superalloys. Philosophical Magazine 90, 375-404.
Ghighi, J., Cormier, J., Ostoja-Kuczynski, E., Mendez, J., Cailletaud, G., Azzouz, F., 2012. A microstructure sensitive approach for the prediction of the creep behavior and life under complex loading paths. Technishe Mechanik 32, 205-220.
Ghosh, R.N., Curtis, R.V., McLean, M., 1990. Creep deformation of single crystal superalloys - Modelling the crystallographic anisotropy. Acta Metall. Mater. 38, 1977-1992.
Glaessgen, E., Stargel, D., 2012. The Digital Twin Paradigm for Future NASA and U.S. Air Force Vehicles, 53rd Structures, Structural Dynamics and Materials Conference. AIAA.
Gurson, A.L., 1975. Plastic flow and fracture behavior of ductile materials incorporating void nucleation, growth, and interaction. Brown University.
Harikrishnan, R., 2021. Microstructure Instabilities in Ni-based single-crystal Superalloys, Aerospace. Texas A&M University.
Harikrishnan, R., Chaugule, P., Dominic, J., le Graverend, J.B., 2021. Multi-axial high-temperature creep in a Ni-based single-crystal superalloy. To be submitted in Acta Materialia.
Harikrishnan, R., le Graverend, J.-B., 2018. A creep-damage phase-field model: Predicting topological inversion in Ni-based single crystal superalloys. Mater. Design 160, 405-416.
Harikrishnan, R., le Graverend, J.-B., 2021. Dependence of Crystallographic Orientation on the Microstructural Evolution and Performance of Ni-based Single Crystal Superalloys: A Phase-Field Informed Crystal Plasticity Study. To be submitted in Materials & Design.
Hayhurst, D.R., Felce, I.D., 1986. Creep rupture under tri-axial tension. Eng. Frac. Mech. 25, 645-664.
Hayhurst, D.R., Leckie, F.A., Morrison, C.J., 1978. Creep Rupture of Notched Bars. Proceedings of the Royal Society of London. Series A, Mathematical and Physical Sciences 360, 243-264.
Hong, H.U., Choi, B.G., Kim, I.S., Yoo, Y.S., Jo, C.Y., 2011. Characterization of deformation mechanisms during low cycle fatigue of a single crystal nickel-based superalloy. J Mater Sci 46, 5245-5251.
Hussain, N., Shahid, K.A., Khan, I.H., Rahman, S., 1995. Oxidation of high-temperature alloys (superalloys) at elevated temperatures in air. II. Oxidation of Metals 43, 363-378.
Ignat, M., Buffiere, J.Y., Chaix, J.M., 1993. Microstructures induced by a stress gradient in a nickel-based superalloy. Acta Metall. Mater. 41, 855-862.
Jacques, A., Diologent, F., Bastie, P., 2004. In situ measurement of the lattice parameter mismatch of a nickel-base single-crystalline superalloy under variable stress. Mater. Sci, Eng. A 387–389, 944-949.
Kachanov, L.M., 1958. Time of the rupture process under creep conditions. Izvestiya Akademii Nauk SSSR. Otdelenie Tekhnicheskikh Nauk 8, 26-31.
Law, C., Blackburn, M.J., 1980. Notch-rupturf behavior of a nickel-base superalloy at intermediate temperatures, International Conference on Superalloys, Seven Spring, PA.
le Graverend, J.-B., 2018. A Lattice-Misfit-Dependent Damage Model for Non-linear Damage Accumulations Under Monotonous Creep in Single Crystal Superalloys. Metall. Mat. Trans. A 49, 4126-4133.
le Graverend, J.-B., 2019. A hardening-based damage model for fast-evolving microstructures: Application to Ni-based single crystal superalloys. International Journal of Plasticity 123, 1-21.
le Graverend, J.-B., Cormier, J., Gallerneau, F., Kruch, S., Mendez, J., 2014a. Highly non-linear creep life induced by a short close γ′-solvus overheating and a prior microstructure degradation on a nickel-based single crystal superalloy. Mater. Design 56, 990-997.
le Graverend, J.-B., Cormier, J., Gallerneau, F., Villechaise, P., Kruch, S., Mendez, J., 2014b. A microstructure-sensitive constitutive modeling of the inelastic behavior of single crystal nickel-based superalloys at very high temperature. International Journal of Plasticity 59, 55-83.
le Graverend, J.-B., Cormier, J., Jouiad, M., Gallerneau, F., Paulmier, P., Hamon, F., 2010. Effect of fine γ' precipitation on non-isothermal creep and creep-fatigue behaviour of nickel base superalloy MC2. Mat. Sci. Eng. A 527, 5295-5302.
le Graverend, J.-B., Dirand, L., Jacques, A., Cormier, J., Ferry, O., Schenk, T., Gallerneau, F., Kruch, S., Mendez, J., 2012. In situ measurement of the γ/γ' lattice mismatch evolution of a nickel-based single-crystal

superalloy during non-isothermal very high-temperature creep experiments. Metall. Mat. Trans. A 43, 3946-3951.
le Graverend, J.-B., Harikrishnan, R., 2019. Finite-Element Crystal Plasticity on Phase-Field Microstructures: Predicting Mechanical Response Variations in Ni-Based Single-Crystal Superalloys. JOM 71, 2600-2611.
le Graverend, J.-B., Harikrishnan, R., 2021. A Lattice-misfit-dependent Micromechanical Approach in Ni-based Single Crystal Superalloys. International Journal of Mechanical Sciences 195, 106229.
le Graverend, J.-B., Lee, S., 2020a. Phenomenological Modeling of the Effect of Oxidation on the Creep Response of Ni-Based Single-Crystal Superalloys, International Symposium on Superalloys. Springer International Publishing, pp. 282-291.
le Graverend, J.-B., Lee, S., 2020b. Phenomenological modeling of the effect of oxidation on the creep response of Ni-based single-crystal superalloys. Extreme Mechanics Letters 39, 100791.
le Graverend, J.-B., Pettinari-Sturmel, F., Cormier, J., Hantcherli, M., Villechaise, P., Douin, J., 2018. Mechanical twinning in Ni-based single crystal superalloys during multiaxial creep at 1050 °C. Mater. Sci, Eng. A 722, 76-87.
le Graverend, J.B., (Harikrishnan, R., 2021. Phase-Field-Informed Vectorial Modeling of Rafting in Ni-based Single Crystal Superalloys. To be submitted in International Journal of Plasticity.
Lee, S., 2019. Instabilities on High Temperature Isothermal Creep Performance in Ni-Based Single Crystal Superalloys, Aerospace Engineering. Texas A&M University.
Lemaitre, J., 1985. A Continuous Damage Mechanics Model for Ductile Fracture. Journal of Engineering Materials and Technology 107, 83-89.
Li, J.R., Zhao, J.Q., Liu, S.Z., Han, M., 2008. Effects of low angle boundaries on the mechanical properties of single crystal superalloy DD6, International Conference on Superalloys, pp. 443-451.
Lukáš, P., Preclík, P., Čadek, J., 2001a. Notch effects on creep behaviour of CMSX-4 superalloy single crystals. Mater. Sci, Eng. A 298, 84-89.
Lukáš, P., Preclík, P., Čadek, J., 2001b. Notch effects on creep behaviour of CMSX-4 superalloy single crystals. Mater. Sci, Eng. A 298, 84-89.
MacLachlan, D.W., Wright, L.W., Gunturi, S., Knowles, D.M., 2001. Constitutive modelling of anisotropic creep deformation in single crystal blade alloys SRR99 and CMSX-4. International Journal of Plasticity 17, 441-467.
Matan, N., Cox, D.C., Carter, P., Rist, M.A., Rae, C.M.F., Reed, R.C., 1999a. Creep of CMSX-4 superalloy single crystals: Effects of misorientation and temperature. Acta Materiala 47, 1549-1563.
Matan, N., Cox, D.C., Rae, C.M.F., Reed, R.C., 1999b. On the kinetics of rafting in CMSX-4 superalloy single crystals. Acta Materialia 47, 2031-2045.
Mattiello, A., 2018. Visco-plasticity and damage modeling of single crystal superalloys at high temperatures : a tensorial microstructure-sensitive approach. ENS Cahcan.
Mattiello, A., Desmorat, R., Cormier, J., 2018. Rate dependent ductility and damage threshold:application to Nickel-based single crystal CMSX-4. Accepted for publication in International Journal of Plasticity.
Méric, L., Cailletaud, G., 1991. Single Crystal Modeling for Structural Calculations: Part 2—Finite Element Implementation. J. Eng. Mater. Technol. 113, 171-182.
Mohles, V., Ronnpagel, D., Nembach, E., 1999. Simulation of dislocation glide in precipitation hardened materials. Comp. Mat. Sci. 16, 144-150.
Nathal, M.V., Mackay, R.A., 1987. The stability of lamellar γ-γ′ structures. Mater. Sci. Eng. 85, 127-138.
Needleman, A., Tvergaard, V., 1984. An analysis of ductile rupture in notched bars. Journal of the Mechanics and Physics of Solids 32, 461-490.
Ott, M., Mughrabi, H., 1999. Dependence of the high-temperature low-cycle fatigue behaviour of the monocrystalline nickel-base superalloys CMSX-4 and CMSX-6 on the γ/γ′-morphology. Mater. Sci, Eng. A 272, 24-30.
Pei, H., Wen, Z., Li, Z., Zhang, Y., Yue, Z., 2018. Influence of surface roughness on the oxidation behavior of a Ni-4.0Cr-5.7Al single crystal superalloy. Applied Surface Science 440, 790-803.

Pessah-Simonetti, M., Caron, P., Khan, T., 1993. Effect of a long-term prior aging on the tensile behavior of a high-performance single crystal superalloy. J. Phys. IV 3, 347-350.
Pollock, T.M., Argon, A.S., 1994. Directional coarsening in nickel-base single crystals with high volume fractions of coherent precipitates. Acta Metall. Mater. 42, 1859-1874.
Potirniche, G.P., Horstemeyer, M.F., Ling, X.W., 2007. An internal state variable damage model in crystal plasticity. Mechanics of Materials 39, 941-952.
Rae, C.M.F., Karunaratne, M.S.A., Small, C.J., Broomfield, R.W., Jones, C.N., Reed, R.C., 2000. TCP phases in an experimental rhenium-containing single crystal superalloy, in: Pollock, T.M., Kissinger, R.D., Bowmann, R.R. (Eds.), International Symposium on Superalloys. TMS, pp. 767-776.
Raffaitin, A., Monceau, D., Crabos, F., Andrieu, E., 2007. The effect of thermal cycling on the high-temperature creep behavior of a single crystal nickel-based superalloy. Scripta Materialia 56, 277-280.
Rajasekharan, R., Petrov, E., 2019. Uncertainty and global sensitivity analysis of bladed disk statics with material anisotropy and root geometry variations. Engineering Reports 1, e12043.
Rajasekharan, R., Petrov, E.P., 2018. Analysis of Deformation of Mistuned Bladed Disks With Friction and Random Crystal Anisotropy Orientation Using Gradient-Based Polynomial Chaos Expansion, ASME Turbo Expo 2018: Turbomachinery Technical Conference and Exposition.
Reuchet, J., Remy, L., 1983. Fatigue oxidation interaction in a superalloy—application to life prediction in high temperature low cycle fatigue. Metallurgical Transactions A 14, 141-149.
Rice, J.R., Tracey, D.M., 1969. On the ductile enlargement of voids in triaxial stress fields∗. Journal of the Mechanics and Physics of Solids 17, 201-217.
Roy Chowdhury, S., Roy, D., 2018. A non-equilibrium thermodynamic model for viscoplasticity and damage: Two temperatures and a generalized fluctuation relation. International Journal of Plasticity.
Sass, V., Feller-Kniepmeier, M., 1998. Orientation dependence of dislocation structures and deformation mechanisms in creep deformed CMSX-4 single crystals. Mater. Sci, Eng. A 245, 19-28.
Sass, V., Glatzel, U., Feller-Kniepmeier, M., 1996. Creep anisotropy in the monocrystalline nickel-base superalloy CMSX-4, in: Kissinger, R.D., others (Eds.), Superalloys. TMS, pp. 283-290.
Steinbach, I., Pezzolla, F., Nestler, B., Seeßelberg, M., Prieler, R., Schmitz, G.J., Rezende, J.L.L., 1996. A phase field concept for multiphase systems. Physica D 94, 135-147.
Stoughton, T.B., Yoon, J.W., 2011. A new approach for failure criterion for sheet metals. International Journal of Plasticity 27, 440-459.
Sugui, T., Jinghua, Z., Huihua, Z., Hongcai, Y., Yongbo, X., Zhuangqi, H., 1999. Aspects of primary creep of a single crystal nickel-base superalloy. Material Science & Engineering A 262, 271-278.
Svoboda, J., Lukas, P., 1998. Model of creep in <001>-oriented superalloy single crystals. Acta. Mater. 46, 3421-3431.
Tinga, T., Brekelmans, W.A.M., Geers, M.G.D., 2009. Directional coarsening in nickel-base superalloys and its effect on the mechanical properties. Comp. Mat. Sci. 47, 471-481.
Tuegel, E.J., Ingraffea, A.R., Eason, T.G., Spottswood, S.M., 2011. Reengineering Aircraft Structural Life Prediction Using a Digital Twin. International Journal of Aerospace Engineering 2011, 14.
Tvergaard, V., 1982. Material failure by void coalescence in localized shear bands. International Journal of Solids and Structures 18, 659-672.
Van Sluytman, J.S., Pollock, T.M., 2012. Optimal precipitate shapes in nickel-base γ-γ' alloys. Acta Materialia 60, 1771-1783.
Véron, M., Bastie, P., 1997. Strain induced directional coarsening in nickel based superalloys: Investigation on kinetics using the small angle neutron scattering (SANS) technique. Acta Materiala 45, 3277-3282.
Viguier, B., Touratier, F., Andrieu, E., 2011. High-temperature creep of single-crystal nickel-based superalloy: microstructural changes and effects of thermal cycling. Philosophical Magazine 91, 4427-4446.
Volkl, R., Glatzel, U., Feller-Kniepmeier, M., 1994. Analysis of matrix and interfacial dislocations in the nickel base superalloy CMSX-4 after creep in [-111] direction. Scripta Metall. Mater. 31, 1481-1486.
Voyiadjis, G.Z., Park, T., 1999. The kinematics of damage for finite-strain elasto-plastic solids. International Journal of Engineering Science 37, 803-830.

Wierzbicki, T., Bao, Y., Lee, Y.-W., Bai, Y., 2005. Calibration and evaluation of seven fracture models. International Journal of Mechanical Sciences 47, 719-743.
Yang, X.L., Lee, P.D., D'Souza, N., 2005. Stray grain formation in the seed region of single-crystal turbine blades. JOM 57, 40-44.
Zghal, J., Gmati, H., Mareau, C., Morel, F., 2016. A crystal plasticity based approach for the modelling of high cycle fatigue damage in metallic materials. International Journal of Damage Mechanics 25, 611-628.
Zhang, J.X., Wang, J.C., Harada, H., Koizumi, Y., 2005. The effect of lattice misfit on the dislocation motion in superalloys during high-temperature low-stress creep. Acta. Mater. 53, 4623-4633.
Zhang, Y., Wen, Z., Pei, H., Zhao, Y., Li, Z., Yue, Z., 2019. Microstructure evolution mechanisms in nickel-based single crystal superalloys under multiaxial stress state. Journal of Alloys and Compounds 797, 1059-1077.
Zhou, H., Ro, Y., Harada, H., Aoki, Y., Arai, M., 2004. Deformation microstructures after low-cycle fatigue in a fourth-generation Ni-base SC superalloy TMS-138. Mater. Sci, Eng. A 381, 20-27.